



A two-step procedure for time-dependent reliability-based design optimization involving piece-wise stationary Gaussian processes

Alexis Cousin¹ · Josselin Garnier² · Martin Guiton³ · Miguel Munoz Zuniga¹

Received: 13 September 2021 / Revised: 23 February 2022 / Accepted: 28 February 2022
© The Author(s), under exclusive licence to Springer-Verlag GmbH Germany, part of Springer Nature 2022

Abstract

We consider in this paper a time-dependent reliability-based design optimization (RBDO) problem with constraints involving the maximum and/or the integral of a random process over a time interval. We focus especially on problems where the process is a stationary or a piece-wise stationary Gaussian process. A two-step procedure is proposed to solve the problem. First, we use ergodic theory and extreme value theory to reformulate the original constraints into time-independent ones. We obtain an equivalent RBDO problem for which classical algorithms perform poorly. The second step of the procedure is to solve the reformulated problem with a new method introduced in this paper and based on an adaptive kriging strategy well suited to the reformulated constraints called AK-ECO for adaptive kriging for expectation constraints optimization. The procedure is applied to two toy examples involving a harmonic oscillator subjected to random forces. It is then applied to an optimal design problem for a floating offshore wind turbine.

Keywords Reliability-based design optimization (RBDO) · Time-dependent reliability · Extreme value theory · Adaptive kriging · Active learning · Monte Carlo

1 Introduction

To ensure the reliability of a structure, it is important to take into account the different sources of uncertainty in the modelling of physical phenomena. For this purpose, uncertainties are usually represented by random variables. In the context of reliability analysis (RA) (Lemaire et al. 2009), failure probability is defined as:

$$\mathbb{P}(g(X_d, X_p, X_r) < 0), \quad (1)$$

where X_d, X_p, X_r are the random variables representing, respectively, the uncertainties of the design variables d , the

model parameters, and the safety thresholds. The function g is called performance function and failure occurs when the function is negative. One evaluation of the performance function often requires a call to a time-consuming simulator. Therefore, the methods proposed in RA aim to evaluate the failure probability accurately and with as few calls to g as possible.

Optimization with a deterministic cost function and constraints expressed as failure probabilities is called reliability-based design optimization (RBDO). The intuitive way to solve a RBDO problem is to couple a classical optimization algorithm and a method to estimate the failure probabilities. This approach is called double-loop since two loops are nested: one estimates the failure probabilities, and the other one updates the design. The reliability index approach (RIA) and the performance measure approach (PMA) (Tu et al. 1999) are among the most popular double-loop approaches. For RIA, the first-order reliability method (FORM) (Madsen et al. 2006) is used to estimate the failure probabilities. In PMA, the initial constraints are replaced by equivalent ones which are evaluated with an inverse reliability analysis. A double-loop strategy can also use a sampling method such as the Monte Carlo approach or one of the variance reduction techniques that require a smaller sample size (El Hami

Responsible Editor: Byeng D. Youn

✉ Alexis Cousin
alexis.cousin@ifpen.fr

¹ IFP Energies Nouvelles, 1-4 Avenue du Bois Préau, 92852 Reuil-Malmaison, France

² CMAP, Ecole Polytechnique, Institut Polytechnique de Paris, 91128 Palaiseau Cedex, France

³ IFP Energies nouvelles, Rond-point de l'échangeur de Solaize, BP 3, 69360 Solaize, France

et al. 2017; Bourinet 2018). In practice, the nesting of the two loops turns out to be very expensive in terms of number of calls to the performance functions.

The single-loop approach (SLA) (Liang et al. 2008; Yang et al. 2020) and the decoupled approaches have been proposed to overcome this drawback. The decoupled approaches consist in solving a sequence of deterministic optimization problems. The final design of an optimization cycle is the starting point of the next one. The sequential optimization and reliability assessment method (SORA) (Du and Chen 2004) separates optimization and reliability loops. A deterministic optimization cycle is carried out for fixed uncertainty values. The latter are then shifted at the next cycle to make the minimum more reliable. Different methods (Torii et al. 2016; Jiang et al. 2020; Wang et al. 2020; Zhang et al. 2021) use the same approach as SORA but propose a different shifting strategy. Benchmarks of the classical reliability approaches have been carried out in Aoues and Chateaneuf (2010) and Lopez and Beck (2012).

In recent years, in the context of RA, many articles have adopted a strategy where the costly performance function is replaced by an approximation model, called metamodel, that is fast to evaluate. Therefore, the failure probability can be estimated with sampling methods since the sample size is no longer an issue. The estimation of failure probabilities with this approach can lead to large errors if the metamodel fitting is of poor quality. Thus, an initial calibration of the metamodel is usually followed by an adaptive enrichment procedure (also called active learning). A learning function makes it possible to select optimal points in the input space of the performance function where the fitting of the metamodel must be improved. In RA, many adaptive procedures have been proposed and vary according to the choice of metamodel, learning function and enrichment stopping criterion. An extensive review and a comparison of these adaptive approaches are detailed in Teixeira et al. (2021).

Metamodels have also been applied to solve RBDO problems. In Dubourg (2011), the performance functions are replaced by kriging models (Krige 1951; Rasmussen 2004) which are enriched during the optimization algorithm. Kriging models with different enrichment strategies are also used in Wu et al. (2021); Li et al. (2020). In Shang et al. (2021), a combination of the polynomial chaos expansion (PCE) (Wiener 1938) and radial basis functions (RBF) (Buhmann 2003) is preferred and is enriched before performing a gradient-based optimization to solve the RBDO problem. A general modular framework is proposed in Moustapha and Sudret (2019) to solve RBDO problem with metamodels: the user can choose the adaptive metamodel, the reliability analysis method, and the optimization algorithm.

Other approaches combine metamodels with PMA, SORA (Zhang et al. 2020b), or SLA (Zhang et al. 2020a). The method proposed in Stieng and Muskulus (2020) that

we will call the Stieng method can deal with general RBDO problems under the assumption that the performance function can be approximated by the product of two functions: one depending only on the design variables which is the performance function evaluated at the mean values of the uncertainties and the other one depending on the uncertain variables. A metamodel is fitted on the second function. The RBDO problem is then solved with sequential cycles of optimization. Each cycle is composed of the update of the metamodels and a resolution with PMA of the problem.

In time-dependent reliability analysis (t-RA), the performance function involves a time-dependent stochastic process denoted \mathcal{Y} . The failure probability is usually written as follows:

$$\mathbb{P}(\exists t \in [0, T], g(X_d, X_p, X_r, \mathcal{Y}(t), t) < 0). \quad (2)$$

The methods estimating this quantity can be classified into the outcrossing approach and the extreme performance approach. The first one provides an upper bound of the failure probability that requires the estimation of an outcrossing rate which can be obtained in several ways (Hawchar 2017). In the PHI2 method (Andrieu-Renaud et al. 2004), the outcrossing rate for a given time t is obtained by performing two reliability analyses with FORM at t and $t + \Delta t$. When \mathcal{Y} is stationary, the outcrossing rate needs to be estimated at only one time t whereas multiple evaluations are required for the non-stationary case. On the other hand, the extreme performance approaches directly provide an estimation of the failure probability. A common way to proceed is to consider the random variable $G_{\min} = \min_{[0, T]} g(X_d, X_p, X_r, \mathcal{Y}(t), t)$ and the probability (2) can then be obtained with a RA method (Hawchar 2017; Hu and Du 2015). Others methods based on adaptive kriging have been proposed and rely on different metamodel strategies (Hu et al. 2020; Wang and Chen 2016; Jiang et al. 2019). For all of these methods, a sequential enrichment strategy is usually performed to improve the accuracy of the metamodel. The failure probability is then computed with Monte Carlo based on the metamodel or with other sampling methods (Ling et al. 2019).

The time-variant reliability-based design optimization (t-RBDO) methods seek to solve optimization problems with constraints involving failure probabilities expressed as in (2). The most straightforward approach to solve a t-RBDO problem is to couple an optimization algorithm with a t-RA method to estimate the constraints at each iteration of the optimization problem (Hawchar 2017). In TROSK (Hawchar et al. 2018) and in PSO-t-IRS (Li and Chen 2019), a kriging model of the performance function is built and enriched over all the design space and then the resolution of the optimization is done using Monte Carlo with the metamodel. Finally, t-SORA and t-SLA are introduced in Shi et al. (2020) and represent the time-variant versions of SORA and SLA.

This paper is motivated by an optimal design problem that aims at minimizing the material cost of the mooring system of a floating offshore wind turbine under fatigue limit state reliability constraints. The structure (the wind turbine) is subjected to random loads due to environmental conditions (wind and waves) which leads to constraints expressed as time-dependent failure probabilities (Cousin et al. 2021). These failure probabilities are more complicated to estimate than the usual ones in t-RA and t-RBDO since the distribution of the time-dependent process involved in our problem depends on random variables. The methods cited above do not suppose any assumption about the process \mathcal{Y} . However, in some applications, such as the one that motivates our work, for fixed values of X_d , X_p and X_r , the performance function is a time-dependent process with known distribution. In offshore engineering, the wind speed and sea elevation are usually represented as stationary or piece-wise stationary Gaussian processes (Vorpahl et al. 2013). When the linearization of the movement equation is a reasonable approximation, quantities of interest such as the displacement of the structure inherit the stationary and Gaussian properties of the input processes.

This linearization implies that the problem considered is in the scope of uncertain linear systems subjected to a stochastic loading for which specific approaches have been proposed to estimate the probability of failure (Valdebenito et al. 2014), for reliability sensitivity estimation (Valdebenito et al. 2012) and for t-RBDO problems as well (Jensen et al. 2008; Jerez et al. 2022). They rely on a discretization of the random excitation and on an adapted sampling method but we will see that a different approach is proposed in this paper.

Motivated by the wind turbine problem, we focus in this paper on t-RBDO with stationary and piece-wise stationary Gaussian processes appearing in two types of constraints: one involving the extreme value of a process and another one, not usually addressed in t-RA and t-RBDO, which involves the integral over time of a process. Instead of following the classical approaches in t-RBDO, we propose a two-step procedure better suited to the characteristics of the studied problem. The first contribution of this article is to use ergodic theory and extreme value theory to reformulate the initial constraints into time-independent ones that are much easier to evaluate. This first part of the procedure is described in Sect. 1 for the stationary case and in Sect. 2 when a piece-wise stationary process is involved. At this stage, we obtain a RBDO problem with specific properties that make existing RBDO approaches suboptimal. Hence, we propose in Sect. 3, a new adaptive kriging strategy called adaptive kriging for expectation constraints optimization (AK-ECO) to solve the reformulated problem efficiently. To illustrate the methodology introduced in this paper, we study two academic cases of a harmonic oscillator presenting the same characteristics as the industrial offshore wind turbine

optimization problem. The numerical results obtained with AK-ECO on the oscillator cases as well as a comparison with state-of-the-art algorithms are presented in Sects. 4 and 5. Our approach is then applied in Sect. 6 to the offshore wind turbine optimization problem.

2 Constraints defined in terms of a stationary Gaussian process

Note 1 In this article, the notations \mathbb{P}_X and \mathbb{E}_X mean that the probability and the expectation are considered with respect to the distribution of X (X can be a random variable, a random vector, a random process, or a combination of the latter).

2.1 Definition of the extreme-based and integral-based constraints

Throughout this paper, we consider a t-RBDO problem of the following form:

$$\begin{aligned} \min_{d \in \Omega_d} \text{cost}(d) \quad \text{such that} \\ \mathbb{P}_{X_d, X_p, X_{r_E}, \mathcal{Y}} \left(\min_{t \in [0, T]} g_E(X_{r_E}, \mathcal{Y}(X_d, X_p; t)) < 0 \right) < p_s \\ \mathbb{P}_{X_d, X_p, X_{r_I}, \mathcal{Y}} \left(\int_0^T g_I(X_{r_I}, \mathcal{Y}(X_d, X_p; t)) dt < 0 \right) < p_s. \end{aligned} \quad (3)$$

In the above equation, the cost function is deterministic and depends on design variables gathered in the vector d . The design space is denoted Ω_d and is a subset of \mathbb{R}^{n_d} . The uncertainties on the design variables, on the model and on the resistance thresholds, are, respectively, represented by the random vectors X_d , X_p , X_{r_E} , and X_{r_I} which are assumed to have known probability density functions. The performance functions are defined by:

$$g_E(X_{r_E}, \mathcal{Y}(X_d, X_p; t)) = X_{r_E} - \mathcal{Y}(X_d, X_p; t), \quad (4)$$

$$g_I(X_{r_I}, \mathcal{Y}(X_d, X_p; t)) = X_{r_I} - f(\mathcal{Y}(X_d, X_p; t)), \quad (5)$$

where $f: \mathbb{R} \rightarrow \mathbb{R}$ is measurable. The time-dependent process is denoted $\mathcal{Y}(x_d, x_p; \cdot)$ and its distribution depends on the outcomes of the random vectors X_d and X_p . The constraints are met if the failure probabilities do not exceed the failure probability threshold p_s .

We will call extreme-based (resp. integral-based) constraint, constraints expressed as the first (resp. second) constraint of problem (3). The failure probability involved in an extreme-based (resp. integral-based) constraint will be denoted $p_E(d)$ (resp. $p_I(d)$) and will be called extreme-based (resp. integral-based) failure probability. Extreme-based failure probability refers to the usual failure probability in t-RBDO except that the process distribution of \mathcal{Y} depends on the random vectors X_d

and X_p . The integral-based failure probability is less studied in t-RBDO and represents the probability that the accumulation of a quantity depending on \mathcal{Y} exceeds some threshold over the time interval $[0, T]$. In the industrial applications we are concerned with (i.e. offshore wind turbines), the evaluation of the functions g_E and g_I is costly, the time T is large and the probability threshold p_s is small.

In t-RBDO, methods used to estimate failure probabilities are often time-consuming as they require numerous evaluations of the performance functions. Under the hypothesis that for fixed values x_d, x_p , the process $\mathcal{Y}(x_d, x_p; \cdot)$ is a stationary or a piece-wise stationary Gaussian process, the first contribution of this article is to show that it is possible to reformulate $p_E(d)$ and $p_I(d)$ as expectations depending only on X_d, X_p, X_{r_E} , and X_{r_I} . Therefore, we obtain an optimization problem much easier to solve. Indeed, the extreme-based failure probability can be written:

$$p_E(d) = \mathbb{E}_{X_d, X_p, X_{r_E}} \left[\mathbb{P}_{\mathcal{Y}(x_d, x_p, X_{r_E})} \left(\min_{t \in [0, T]} g_E(X_{r_E}, \mathcal{Y}(x_d, x_p; t)) < 0 \right) \right] \quad (6)$$

and we will show that, for fixed values of X_d, X_p, X_{r_E} and when T is large, limit theorems for functionals of stationary or piece-wise stationary processes provide a good approximation of the conditional probability $\mathbb{P}_{\mathcal{Y}}(\min_{t \in [0, T]} g_E(X_{r_E}, \mathcal{Y}(x_d, x_p; t)) < 0)$. Furthermore, this approximation only uses the spectral properties of $\mathcal{Y}(x_d, x_p; \cdot)$ and the resulting constraint is much easier to evaluate since it does not require any additional evaluation of \mathcal{Y} and only depends on the random vectors X_d, X_p , and X_{r_E} . The same reasoning will be applied to give an approximation of the integral-based failure probability.

For fixed values x_d and x_p , we consider in this section that the process $\mathcal{Y}(x_d, x_p; \cdot)$ is a stationary Gaussian process with zero mean. Its distribution is defined by its spectral density $K_{\mathcal{Y}}(x_d, x_p; \cdot)$ which is the Fourier transform of its autocorrelation function $k_{\mathcal{Y}}(x_d, x_p; \cdot)$ that depends on x_d and x_p :

$$K_{\mathcal{Y}}(x_d, x_p; \omega) = \frac{1}{2\pi} \int_{\mathbb{R}} k_{\mathcal{Y}}(x_d, x_p; t) e^{-i\omega t} dt. \quad (7)$$

The spectral moment of order n of $\mathcal{Y}(x_d, x_p; \cdot)$ is defined as:

$$m_{\mathcal{Y}, n}(x_d, x_p) = \int_{\mathbb{R}} \omega^n K_{\mathcal{Y}}(x_d, x_p; \omega) d\omega. \quad (8)$$

2.2 Approximation of the extreme-based failure probability

For fixed values of X_d, X_p, X_{r_E} , and with g_E defined in (4), the probability $\mathbb{P}_{\mathcal{Y}}(\min_{t \in [0, T]} g_E(X_{r_E}, \mathcal{Y}(x_d, x_p; t)) < 0)$ involves the extremum of a stationary Gaussian process.

Thus, the extreme value theory (Leadbetter et al. 1983) and especially the following theorem are well suited to provide a reformulation of $p_E(d)$. We present a slightly modified version of the theorem 8.2.7 of Leadbetter et al. (1983) for a stationary Gaussian process $\{\xi(t); t \geq 0\}$ with zero mean, autocorrelation function k_{ξ} , spectral density K_{ξ} and spectral moment of order n denoted $m_{\xi, n}$.

Theorem 1 Suppose that the Gaussian stationary process ξ has non-zero spectral moments $m_{\xi, 0}$ and $m_{\xi, 2}$ and satisfies the following conditions:

$$k_{\xi}(\tau) = m_{\xi, 0} - \frac{m_{\xi, 2}\tau^2}{2} + o(\tau^2) \text{ as } \tau \rightarrow 0, \quad (9)$$

$$k_{\xi}(\tau) \log(\tau) \rightarrow 0 \text{ as } \tau \rightarrow \infty, \quad (10)$$

then, as $T \rightarrow +\infty$,

$$\mathbb{P} \left(a_T \left(\max_{t \in [0, T]} \frac{\xi(t)}{\sqrt{m_{\xi, 0}}} - a_T \right) \leq x \right) \rightarrow \exp(-e^{-x}), \quad (11)$$

with $a_T = \sqrt{2 \log(T/T_c)}$ and $T_c = 2\pi \sqrt{m_{\xi, 0}/m_{\xi, 2}}$.

The formulation of theorem 1 of this paper is obtained by applying theorem 8.2.7 of Leadbetter et al. (1983) to the process $\xi(tT_c)$.

Remark 1 It is possible to give sufficient conditions for theorem 1 that are explicit in K_{ξ} . Denoting K'_{ξ} the derivative of K_{ξ} , conditions (9) and (10) are met if we have:

$$m_{\xi, 0} < \infty, m_{\xi, 2} < \infty, \quad (12)$$

$$K_{\xi} \in C^1, K_{\xi} \text{ and } K'_{\xi} \text{ are integrable.} \quad (13)$$

For condition (13), we use that if $K_{\xi} \in C^1$ and K_{ξ} and K'_{ξ} are integrable then $\exists c > 0$ such that $|k_{\xi}(\tau)| \leq \frac{c}{|\tau|}$ and therefore, condition (10) is met. Other sufficient conditions on the spectral density are discussed in Berman (1991).

For fixed values x_d and x_p , if the process $\mathcal{Y}(x_d, x_p; \cdot)$ introduced in Sect. 1.1 meets conditions (12) and (13), we can apply theorem 1 and obtain $\forall x$, as $T \rightarrow +\infty$:

$$\mathbb{P}_{\mathcal{Y}} \left(a_T(x_d, x_p) \left(\max_{t \in [0, T]} \frac{\mathcal{Y}(x_d, x_p; t)}{\sqrt{m_{\mathcal{Y}, 0}(x_d, x_p)}} - a_T(x_d, x_p) \right) \leq x \right) \rightarrow \exp(-e^{-x}), \quad (14)$$

with $a_T(x_d, x_p) = \sqrt{2 \log \left(\frac{T}{2\pi} \sqrt{\frac{m_{\mathcal{Y},2}(x_d, x_p)}{m_{\mathcal{Y},0}(x_d, x_p)}} \right)}$. Therefore, for T large enough, it is reasonable to make the following approximation:

$$p_E(d) \simeq \mathbb{E}_{X_d, X_p, X_E} \left[F_e \left(\exp \left(a_T(X_d, X_p)^2 - \frac{a_T(X_d, X_p) X_{r_E}}{\sqrt{m_{\mathcal{Y},0}(X_d, X_p)}} \right) \right) \right], \quad (15)$$

with $F_e(x) = 1 - \exp(-x)$. The approximation error made in equation (15) can be bounded with classical results (Kratz and Rootzén 1997) and is discussed in Sect. A.1 of Appendix A.

Remark 2 The initial failure probability that depends on a random process has been approximated by an expectation which only depends on random vectors. Furthermore, to compute the quantity within the square brackets in (15), only two spectral moments of $\mathcal{Y}(x_d, x_p; \cdot)$ need to be evaluated (for each outcome of X_d and X_p).

2.3 Approximation of the integral-based failure probability

We focus now on $p_I(d)$. For fixed values x_d, x_p , the process $f(\mathcal{Y}(x_d, x_p; \cdot))$ is denoted by $\mathcal{F}(x_d, x_p; \cdot)$. Since $\mathcal{Y}(x_d, x_p; \cdot)$ is stationary, $\mathcal{F}(x_d, x_p; \cdot)$ is also stationary and we denote by $k_{\mathcal{F}}(x_d, x_p; \cdot)$ its autocovariance function. In the following, we will use the definition of ergodicity below.

Definition 1 The process $\mathcal{F}(x_d, x_p; \cdot)$ is said to be ergodic if:

$$\frac{1}{T} \int_0^T \mathcal{F}(x_d, x_p; t) dt \xrightarrow[T \rightarrow +\infty]{\mathbb{P}} \mathbb{E}_{\mathcal{F}}[\mathcal{F}(x_d, x_p; 0)], \quad (16)$$

where $\xrightarrow{\mathbb{P}}$ refers to the convergence in probability. A sufficient condition for the stationary process $\mathcal{F}(x_d, x_p; \cdot)$ to be ergodic [cf Sect. 13.1 of Papoulis (1991)] is that $k_{\mathcal{F}}(x_d, x_p; \cdot)$ is integrable.

Suppose that $\mathcal{F}(x_d, x_p; \cdot)$ is ergodic. Then, for almost every x (more exactly $\forall x \neq \mathbb{E}_{\mathcal{F}}[\mathcal{F}(x_d, x_p; 0)]$):

$$\mathbb{P}_{\mathcal{Y}} \left(\frac{1}{T} \int_0^T \mathcal{F}(x_d, x_p; t) dt > x \right) \rightarrow \mathbb{1}_{\mathbb{E}_{\mathcal{F}}[\mathcal{F}(x_d, x_p; 0)] > x}, \quad (17)$$

as $T \rightarrow +\infty$. Thus, for T large enough, it is reasonable to approximate the integral-based failure probability as follows:

$$p_I(d) \simeq \mathbb{E}_{X_d, X_p} [F_{r_1}(T \mathbb{E}_{\mathcal{F}}[\mathcal{F}(X_d, X_p; 0)])], \quad (18)$$

with F_{r_1} the cumulative distribution function of X_{r_1} (which is continuous). The approximation error made in equation (18) is discussed in Sect. A.2 of Appendix A.

Remark 3 To compute $\mathbb{E}_{\mathcal{F}}[\mathcal{F}(x_d, x_p; 0)]$, it is necessary to know the distribution of $\mathcal{Y}(x_d, x_p; 0)$. Since the process $\mathcal{Y}(x_d, x_p; \cdot)$ is Gaussian with zero mean, the variance of $\mathcal{Y}(x_d, x_p; 0)$ determines its distribution. Hence, to compute the quantity within the square brackets in (18), we only need to know the variance of $\mathcal{Y}(x_d, x_p; 0)$ for each outcome of X_d and X_p .

2.4 Optimization problem involving a stationary harmonic oscillator

We present in this section a concrete optimization problem with constraints involving extreme-based and integral-based failure probabilities and we apply the reformulation procedure described in Sects. 1.2 and 1.3.

Let us consider a harmonic oscillator on an interval of time $[0, T]$: a spring/mass system. We denote, respectively, by x_{d_1} the mass of the object, x_{d_2} the spring stiffness, and x_p the damping coefficient. An external force is exerted on the system. To account for all the sources of uncertainty of the experiment, the values of x_{d_1} , x_{d_2} , x_p and the external force are considered random. These uncertainties are, respectively, represented by the random variables X_{d_1} , X_{d_2} , X_p , and the stochastic process $\eta(t)$. We denote X_d the random vector (X_{d_1}, X_{d_2}) of outcome $x_d = (x_{d_1}, x_{d_2})$ whose distribution depends on the design variable $d = (d_1, d_2)$.

Consequently, for fixed values x_d and x_p , the displacement of the mass with respect to the equilibrium position is represented by a stochastic process denoted $\mathcal{D}(x_d, x_p; \cdot)$ which is solution of the harmonic oscillator equation:

$$x_{d_1} \mathcal{D}^{(2)}(x_d, x_p; t) + x_p \mathcal{D}^{(1)}(x_d, x_p; t) + x_{d_2} \mathcal{D}(x_d, x_p; t) = \eta(t), \quad t \in [0, T], \quad (19)$$

where $\mathcal{D}^{(1)}(x_d, x_p; \cdot)$ and $\mathcal{D}^{(2)}(x_d, x_p; \cdot)$ are, respectively, the velocity and acceleration processes whose sample paths are the first and second time derivatives of the sample path of $\mathcal{D}(x_d, x_p; \cdot)$.

The optimization problem consists in minimizing a linear function $cost(d)$ while constraints are imposed on the design variable such that:

- the velocity and the acceleration of the oscillator must stay below given thresholds x_{r_1} and x_{r_2} , respectively (this is a simplified model for the extreme constraints that we have in mind in our industrial application);
- the accumulated amount of acceleration of the object exceeding the threshold ρ must remain under a resistance

threshold x_{r_3} (this is a simplified model for the fatigue constraint that we have in mind in our industrial application).

The thresholds $x_{r_1}, x_{r_2}, x_{r_3}$ are also random and therefore outcomes of random variables denoted X_{r_1}, X_{r_2} , and X_{r_3} . The optimization problem is formulated as follows:

$$\begin{aligned} \min_{d \in \Omega_d} \text{cost}(d) \quad \text{such that} \\ \mathbb{P}_{X_d, X_p, X_{r_k}, \eta} \left(\max_{t \in [0, T]} \mathcal{D}^{(k)}(X_d, X_p; t) > X_{r_k} \right) < p_s, \\ k = 1, 2 \\ \mathbb{P}_{X_d, X_p, X_{r_3}, \eta} \left(\int_0^T \left(\left| \mathcal{D}^{(2)}(X_d, X_p; t) \right| - \rho \right)^+ dt > X_{r_3} \right) < p_s \end{aligned} \quad (20)$$

with $x^+ = \max(0, x)$. The design space is defined as $\Omega_d = [d_1^-, d_1^+] \times [d_2^-, d_2^+] \subset \mathbb{R}^2$. The distributions of X_d and X_p are chosen such that the oscillator is under-damped for almost all realizations i.e. $X_p^2 - 4X_{d_1}X_{d_2} < 0$ almost surely. Moreover, we assume that the process η is stationary, Gaussian with spectral density $K_\eta(\omega) = \frac{\theta}{\sqrt{2\pi}} \exp\left(-\frac{(\theta\omega)^2}{2}\right)$ with $\theta > 0$. Finally, all the sources of uncertainty $(X_{d_1}, X_{d_2}, X_p, X_{r_1}, X_{r_2}, X_{r_3}, \eta)$ are independent.

For fixed values of X_d, X_p , it follows from equation (19) and the stationarity of η (see Lindgren 2012) that the process $\mathcal{D}(x_d, x_p; \cdot)$ is stationary and can be written as the output of a linear filter $\mathcal{D}(x_d, x_p; t) = (h_{\mathcal{D}}(x_d, x_p, \cdot) * \eta)(t)$, with $h_{\mathcal{D}}$ defined by:

$$\begin{aligned} H_{\mathcal{D}}(x_d, x_p; \omega) &= \text{FT}(h_{\mathcal{D}}(x_d, x_p; \cdot))(\omega) \\ &= \frac{1}{-\omega^2 x_{d_1} + i\omega x_p + x_{d_2}} \end{aligned} \quad (21)$$

where FT refers to the Fourier transformation. It is shown (see Lindgren 2012) that the process $\mathcal{D}(x_d, x_p; \cdot)$ is then also Gaussian with zero mean and its spectral density is given by:

$$K_{\mathcal{D}}(x_d, x_p; \omega) = \left| H_{\mathcal{D}}(x_d, x_p; \omega) \right|^2 K_\eta(\omega). \quad (22)$$

Furthermore, if the process $\mathcal{D}(x_d, x_p; \cdot)$ has finite spectral moment of order 2 and 4 (see theorem 2.2 of Lindgren 2012), the processes $\mathcal{D}^{(1)}(x_d, x_p; \cdot)$ and $\mathcal{D}^{(2)}(x_d, x_p; \cdot)$ are also zero-mean stationary Gaussian processes with spectral densities, denoted, respectively, $K_{\mathcal{D}^{(1)}}(x_d, x_p, \cdot)$ and $K_{\mathcal{D}^{(2)}}(x_d, x_p, \cdot)$, given by:

$$K_{\mathcal{D}^{(k)}}(x_d, x_p; \omega) = \omega^{2k} K_{\mathcal{D}}(x_d, x_p; \omega) \quad k = 1, 2. \quad (23)$$

Remark 4 In fact, the result of theorem 2.2 of Lindgren (2012) holds for the first- and second-order derivatives of $\mathcal{D}(x_d, x_p; \cdot)$ in the quadratic mean sense. But under the supplementary condition that the spectral moment of order 6

of $\mathcal{D}(x_d, x_p; \cdot)$ is also finite, the result holds for sample path derivatives too (see Lindgren 2012).

The spectral moments of order n of $\mathcal{D}^{(k)}(x_d, x_p; \cdot)$ $k = 1, 2$, are denoted $m_{\mathcal{D}^{(k)}, n}(x_d, x_p)$ $k = 1, 2$. It follows from the properties of the processes $\mathcal{D}^{(k)}(x_d, x_p; \cdot)$, $k = 1, 2$ that the two first constraints of problem (20) are extreme-based constraints whereas the third constraint is integral-based. We show in Sect. A.3 in Appendix A that, for all x_d, x_p , the processes $\mathcal{D}^{(k)}(x_d, x_p; \cdot)$, $k = 1, 2$, meet the sufficient conditions (12, 13) which allow the reformulation of the two first constraints of the problem under study. Since the process $\mathcal{D}^{(2)}(x_d, x_p; \cdot)$ is Gaussian and its autocovariance function converges to 0 at infinity and is integrable, it is easy to show that the process $\mathcal{F}(x_d, x_p; \cdot) = \left(\left| \mathcal{D}^{(2)}(x_d, x_p; \cdot) \right| - \rho \right)^+$ has an integrable autocovariance function and thus, $\mathcal{F}(x_d, x_p; \cdot)$ is ergodic.

Since all the required conditions are met, for T large enough, we can apply the reformulation steps described in Sects. 1.2 and 1.3 to the constraints of problem (20). The two first constraints are replaced by the approximation given by (15) where $a_T, m_{\mathcal{Y}, 0}$ and X_{r_E} become, respectively, $a_T^1, m_{\mathcal{D}^{(1)}, 0}$ and X_{r_1} for the first constraint and $a_T^2, m_{\mathcal{D}^{(2)}, 0}$ and X_{r_2} for the second constraint with:

$$a_T^k(x_d, x_p) = \sqrt{2 \log \left(\frac{T}{2\pi} \sqrt{\frac{m_{\mathcal{D}^{(k)}, 2}(x_d, x_p)}{m_{\mathcal{D}^{(k)}, 0}(x_d, x_p)}} \right)}, \quad (24)$$

for $k = 1, 2$. The third constraint of problem (20) is replaced by the approximation given by (18) with

$$\mathcal{F}(x_d, x_p; 0) = \left(\left| \mathcal{D}^{(2)}(x_d, x_p; 0) \right| - \rho \right)^+, \quad (25)$$

and X_{r_1} becomes X_{r_3} .

3 Constraints defined in terms of a piece-wise stationary Gaussian process

3.1 Definition of the piece-wise stationary process

We consider in this section the optimization problem (3) introduced in Sect. 1 with extreme-based and integral-based constraints except that the process \mathcal{Y} is now piece-wise stationary. The period $[0, T]$ is decomposed into n_T intervals $I_i = [(i-1)\Delta T, i\Delta T]$, $i = 1, \dots, n_T$ and for fixed x_d, x_p the process \mathcal{Y} is defined as:

$$\mathcal{Y}(x_d, x_p; t) = \sum_{i=1}^{n_T} \mathcal{Y}_i(x_d, x_p, s_i; t) \mathbb{1}_{I_i}(t) \quad (26)$$

where s_1, \dots, s_{n_T} is a sequence of elements of the set $\{s^1, \dots, s^{n_s}\}$. The processes $\mathcal{Y}_i(x_d, x_p, s_i; \cdot)$, $i = 1, \dots, n_T$, are independent stationary Gaussian processes with zero mean. The distribution of $\mathcal{Y}_i(x_d, x_p, s_i; \cdot)$ for $i \in \{1, \dots, n_T\}$ is defined by its spectral density $K_{\mathcal{Y}}(x_d, x_p, s_i; \cdot)$ and we denote $m_{\mathcal{Y},n}(x_d, x_p, s_i)$ its spectral moment of order n . We denote n^j and p^j , the quantities such that $n^j = \#\{i \in \{1, \dots, n_T\}, s_i = s^j\}$ and $p^j = n^j/n_T$ for $j = 1, \dots, n_s$.

Remark 5 The definitions of the objects introduced in this section are motivated by the industrial case of a floating offshore wind turbine. In this application, each process $\mathcal{Y}_i(x_d, x_p, s^j; \cdot)$ can be seen as the displacement over time of the floating platform subjected to a sea elevation process characterized by a sea state defined by s^j , for some design and parametric variables x_d and x_p . The constraints then relate to the maximum admissible displacement of the structure or to the accumulated damage of the mooring lines. Furthermore, dividing the time interval $[0, T]$ into n_T intervals is standard in offshore models to represent the different sea states encountered during the period $[0, T]$. We can refer, for instance, to Labeyrie (1990) which justifies that 3 hours can be considered as the mean duration of stationarity from data measurements made in North Sea. This duration may differ for another site. Furthermore, one should also consider that due to the limited number of years of measurement and the annual variation of the environmental conditions, the long-term statistics of sea states are uncertain (see Moan et al. 2005). To stay close to the engineering terminology, s^j will be called the state of the process $\mathcal{Y}_i(x_d, x_p, s^j; \cdot)$ in this paper.

The reasoning for extreme-based and integral-based constraints reformulation is the same as for the stationary case: the purpose is to provide good approximations that only rely on spectral properties of the processes $\mathcal{Y}_i(x_d, x_p, s_i; \cdot)$.

3.2 Approximation of the extreme-based failure probability

To approximate the extreme-based failure probability, we claim that, for fixed x_d, x_p, x_{r_E} and for ΔT large enough:

$$\begin{aligned} \mathbb{P}_{\mathcal{Y}}\left(\max_{t \in [0, T]} \mathcal{Y}(x_d, x_p; t) \leq x_{r_E}\right) \\ \simeq \prod_{j=1}^{n_s} \mathbb{P}_{\mathcal{Y}_1}\left(\max_{t \in [0, T p^j]} \mathcal{Y}_1(x_d, x_p, s^j; t) \leq x_{r_E}\right) \end{aligned} \quad (27)$$

This approximation is justified in Sect. B.1 of Appendix B.

Therefore, if for all x_d, x_p, x_{r_E} , and for all states s^j , the process $\mathcal{Y}_1(x_d, x_p, s^j; \cdot)$ meets the conditions of theorem 1, it follows from equation (27) and theorem 1 that for ΔT sufficiently large, we can make the following approximation:

$$\begin{aligned} p_E(d) \simeq \mathbb{E}_{X_d, X_p, X_{r_E}} \\ \left[F_e \left(\sum_{j=1}^{n_s} \exp \left(a_{T p^j}(X_d, X_p, s^j)^2 - \frac{a_{T p^j}(X_d, X_p, s^j) X_{r_E}}{\sqrt{m_{\mathcal{Y},0}(X_d, X_p, s^j)}} \right) \right) \right] \end{aligned} \quad (28)$$

with

$$a_{T p^j}(x_d, x_p, s^j) = \sqrt{2 \log \left(\frac{T p^j}{2\pi} \sqrt{\frac{m_{\mathcal{Y},2}(x_d, x_p, s^j)}{m_{\mathcal{Y},0}(x_d, x_p, s^j)}} \right)}. \quad (29)$$

Bounds on the approximation error of equation (28) are proposed in Sect. B.2 of Appendix B.

3.3 Approximation of the integral-based failure probability

Proposition 1 We denote by $\mathcal{F}_1(x_d, x_p, s^j; \cdot)$ the process $f(\mathcal{Y}_1(x_d, x_p, s^j; \cdot))$. If for all x_d, x_p, s^j , the process $\mathcal{F}_1(x_d, x_p, s^j; \cdot)$ is ergodic, we have for almost every x :

$$\begin{aligned} \mathbb{P}_{\mathcal{Y}}\left(\frac{1}{\Delta T} \int_0^T f(\mathcal{Y}(x_d, x_p; t)) dt > x\right) \\ \xrightarrow[\Delta T \rightarrow +\infty]{} \mathbb{1}_{\sum_{j=1}^{n_s} n^j \mathbb{E}_{\mathcal{F}_1}[\mathcal{F}_1(x_d, x_p, s^j; 0)] > x}. \end{aligned} \quad (30)$$

The proof of proposition 1 is given in Sect. B.3 of Appendix B.

Using proposition 1, when ΔT is large enough, we can approximate the integral-based failure probability as follows:

$$\begin{aligned} p_I(d) \\ \simeq \mathbb{E}_{X_d, X_p} \left[F_{r_1} \left(T \sum_{j=1}^{n_s} p^j \mathbb{E}_{\mathcal{F}_1}[\mathcal{F}_1(X_d, X_p, s^j; 0)] \right) \right], \end{aligned} \quad (31)$$

with F_{r_1} the cumulative distribution function of X_{r_1} . The approximation error made in equation (31) is discussed in Sect. B.4 of Appendix B.

3.4 Optimization problem involving a piece-wise stationary harmonic oscillator

The oscillator problem presented in Sect. 1.4 is slightly modified by considering a piece-wise stationary process \mathcal{D} as defined in Sect. 2.1. For fixed values x_d, x_p and for $i = 1, \dots, n_T$, the process $\mathcal{D}_i(x_d, x_p, s_i; \cdot)$ is solution of the harmonic oscillator equation (19) with an external force $\eta(s_i, \cdot)$. The time-dependent process $\eta(s_i, \cdot)$ is a zero-mean stationary Gaussian process with spectral density:

$$K_\eta(s_i; \omega) = \frac{s_i}{\sqrt{2\pi}} \exp\left(-\frac{(s_i \omega)^2}{2}\right), \quad (32)$$

for $s_i > 0$. In the piece-wise stationary problem, the processes $\mathcal{D}^{(1)}$ and $\mathcal{D}^{(2)}$ are defined by the following equation:

$$\mathcal{D}^{(k)}(x_d, x_p; t) = \sum_{i=1}^{n_T} \mathcal{D}_i^{(k)}(x_d, x_p, s_i; t) \mathbb{1}_{I_i}(t), \quad (33)$$

for $k = 1, 2$, with $\mathcal{D}_i^{(k)}(x_d, x_p, s_i; \cdot)$, the first ($k = 1$) and second ($k = 2$) time derivatives of $\mathcal{D}_i(x_d, x_p, s_i; \cdot)$. Hence, the processes $\mathcal{D}_i^{(k)}(x_d, x_p, s_i; \cdot)$, $k = 1, 2$, are zero-mean stationary Gaussian processes with respective spectral densities:

$$K_{\mathcal{D}^{(k)}}(x_d, x_p, s_i; \omega) = \omega^{2k} |H_{\mathcal{D}}(x_d, x_p; \omega)|^2 K_\eta(s_i; \omega), \quad (34)$$

for $k = 1, 2$. We denote $m_{\mathcal{D}^{(k)}, n}(x_d, x_p, s_i)$, $k = 1, 2$, their spectral moments of order n . Furthermore, the arguments used in the stationary case allow to show that the processes $\mathcal{D}_i^{(k)}(x_d, x_p, s_i; \cdot)$, $k = 1, 2$, meet all the conditions to use the reformulation procedure described in Sect. 2.

If ΔT is large enough, it is reasonable to approximate the constraints of problem (20) with a piece-wise stationary process \mathcal{D} by applying the results of Sects. 2.2 and 2.3. The two first constraints are replaced by the approximation given by equation (28) where a_{Tp^j} , $m_{\mathcal{Y}, 0}$ and X_{r_E} become, respectively, $a_{Tp^j}^1$, $m_{\mathcal{D}^{(1)}, 0}$ and X_{r_1} for the first constraint and $a_{Tp^j}^2$, $m_{\mathcal{D}^{(2)}, 0}$ and X_{r_2} for the second constraint with:

$$a_{Tp^j}^k(x_d, x_p, s^j) = \sqrt{2 \log \left(\frac{Tp^j}{2\pi} \sqrt{\frac{m_{\mathcal{D}^{(k)}, 2}(x_d, x_p, s^j)}{m_{\mathcal{D}^{(k)}, 0}(x_d, x_p, s^j)}} \right)}, \quad (35)$$

for $k = 1, 2$. The third constraint of problem (20) is replaced by the approximation given by equation (31) with

$$\mathcal{F}_1(x_d, x_p, s^j; 0) = \left(|\mathcal{D}_1^{(2)}(x_d, x_p, s^j; 0)| - \rho \right)^+ \quad (36)$$

and X_{r_1} becomes X_{r_3} . We give the relation between $\mathbb{E}_{\mathcal{F}_1}[\mathcal{F}_1(x_d, x_p, s^j; 0)]$ and $m_{\mathcal{D}^{(2)}, 0}(x_d, x_p, s^j)$ in Appendix B.5.

Remark 6 To evaluate $a_{Tp^j}^k(x_d, x_p, s^j)$, $k = 1, 2$ and $\mathbb{E}_{\mathcal{F}_1}[\mathcal{F}_1(x_d, x_p, s^j; 0)]$, the spectral moments of the velocity and acceleration processes need to be numerically computed from the integrals

$$\int_{\mathbb{R}} \omega^n |H_{\mathcal{D}}(x_d, x_p; \omega)|^2 K_\eta(s^j; \omega) d\omega, \quad (37)$$

for $n = 2, 4, 6$. Hence, the evaluation of the spectral moments represents the expensive part of the evaluation of the constraints.

4 An active learning Kriging approach for the reformulated optimization problem: AK-ECO

We consider in this section the general problem (3) introduced in Sect. 1 involving a piece-wise stationary process. After the reformulation of the constraints presented in Sect. 2, we end up with the following problem:

$$\begin{aligned} \min_{d \in \Omega_d} \text{cost}(d) \quad \text{such that} \\ \mathbb{E}_{X_d, X_p, X_{r_E}} \left[F_\epsilon \left(\sum_{j=1}^{n_s} \exp(M_E(X_d, X_p, X_{r_E}, s^j)) \right) \right] < p_s \\ \mathbb{E}_{X_d, X_p} \left[F_{r_1} \left(\sum_{j=1}^{n_s} Tp^j M_1(X_d, X_p, s^j) \right) \right] < p_s \end{aligned} \quad (38)$$

with

$$\begin{aligned} M_E(x_d, x_p, x_{r_E}, s^j) &= a_{Tp^j}(x_d, x_p, s^j)^2 \\ &\quad - \frac{a_{Tp^j}(x_d, x_p, s^j) x_{r_E}}{\sqrt{m_{\mathcal{Y}, 0}(x_d, x_p, s^j)}}, \end{aligned} \quad (39)$$

$$M_1(x_d, x_p, s^j) = \mathbb{E}_{\mathcal{F}_1}[\mathcal{F}_1(x_d, x_p, s^j; 0)]. \quad (40)$$

All the notations appearing in problem (38) have been introduced in Sect. 2. The *cost* function is supposed to be fast to evaluate. We remark that the problem is now a time-independent one. Even though the reformulated constraints are easier to evaluate than the initial ones, for each realization x_d, x_p and for each state s^j , the spectral moments of $\mathcal{Y}_1(x_d, x_p, s^j; \cdot)$ are required to compute the quantities $M_E(x_d, x_p, x_{r_E}, s^j)$ and $M_1(x_d, x_p, s^j)$. The evaluation of those spectral moments requires an expensive simulator. Therefore, an estimation of one of the constraints with the Monte Carlo method and a sample of size n_{MC} would impose $n_{MC} \times n_s$ calls to the simulator. This would be too computationally expensive especially when we deal with rare events (i.e. when $p_s \ll 1$). We mentioned in the introduction of the paper existing methods that solve RBDO problems much faster than the brute Monte Carlo. However, we will see the drawbacks of these methods when applied to problem (38). We thus propose a new method, better suited for the reformulated problem and called adaptive kriging for expectation constraints optimization (AK-ECO).

Remark 7 Presented as in problem (38), the reformulated constraints depend on the same piece-wise stationary process \mathcal{Y} . However, the resolution methods that are presented in this section can be applied to constraints that depend on different processes. When several constraints depend on the same process, it can be noticed that the outputs of each

simulation can be used in the estimation of the different constraints since they depend on the same quantities (i.e. the spectral moments of the process).

Remark 8 For simplicity, we present a problem with two constraints (one extreme-based and one integral-based) but the resolution methods that we introduce can be applied to several constraints of each type. Furthermore, a problem with extreme- and integral-based constraints but with a stationary process \mathcal{Y} can be solved with the same approaches since the reformulated problem would be identical to the piece-wise stationary case considering $n_s = 1$.

All the effective approaches in the literature of RBDO methods rely on the assumption that the constraints are expressed as probabilities. Thus, we write the extreme-based and integral-based reformulated constraints of problem (38) as failure probabilities as follows:

$$\mathbb{P}_{X_d, X_p, X_{r_E}, X_e} \left(X_e - \sum_{j=1}^{n_s} \exp(M_E(X_d, X_p, X_{r_E}, s^j)) < 0 \right) < p_s, \quad (41)$$

$$\mathbb{P}_{X_d, X_p, X_{r_I}} \left(X_{r_I} - \sum_{j=1}^{n_s} T p^j M_I(X_d, X_p, s^j) < 0 \right) < p_s, \quad (42)$$

where X_e is a random variable with an exponential distribution of parameter 1. However, since each evaluation of the functions M_E and M_I requires a call to an expensive simulator, one evaluation of the performance function of each of these constraints would need n_s simulations. When n_s is large, which is the case for offshore applications (Vorpahl et al. 2013), the double-loop, single-loop and decoupled loop approaches can be too expensive. This is also the case for the adaptive metamodel approaches since they always replace the whole performance function.

The limitations of the current methods in RBDO have motivated the development of a new approach. For each expectation constraint of problem (38), a metamodel is built to replace the expensive function involved in the reformulated failure probability. We thus obtain as many metamodels as there are constraints. Then, cycles of optimization are carried out. During each cycle, the metamodels are sequentially enriched and the design point is updated. The particularity of our approach lies in the metamodel and active learning strategy which are adapted to the reformulated constraints of the studied problem.

4.1 Metamodel strategy: Kriging

In problem (38), since the expensive functions of the extreme-based and integral-based constraints are M_E and M_I , we

propose to build a metamodel for each of these functions. Unlike other metamodel approaches, the metamodels do not replace the performance functions. Thus, for each (x_d, x_p, x_{r_E}) , the functions M_E and M_I need to be evaluated only on the relevant state s^j as we will see below. This could drastically reduce the number of calls to the simulator, especially when n_s is large.

As in Dubourg (2011) and Moustapha and Sudret (2019), for each constraint, we build the metamodel in a so-called augmented space which allows to use and enrich a single model during the whole procedure of AK-ECO. To do so, the augmented space spans both the design space and the space of uncertainties. The augmented spaces of M_E and M_I are, respectively, denoted Ω_E^{aug} and Ω_I^{aug} . To define precisely those spaces, we need to introduce some notations.

Let $(d_1, \dots, d_{n_d}) \in \Omega_d = \Omega_{d_1} \times \dots \times \Omega_{d_{n_d}} \subset \mathbb{R}^{n_d}$ be a design point and $X_{d_1}, \dots, X_{d_{n_d}}$ the random variables with respective cumulative distribution functions $F_{d_1}, \dots, F_{d_{n_d}}$ describing the uncertainties at this point. The random vector X_p is composed of n_p random variables X_{p_i} , ($i = 1, \dots, n_p$) with cumulative distribution functions F_{p_i} , ($i = 1, \dots, n_p$). Finally, the cumulative distribution function of X_{r_E} is denoted F_{r_E} . The augmented spaces are then defined as follows:

$$\Omega_E^{aug} = \Omega_d^{aug} \times \Omega_p^{aug} \times \Omega_{r_E}^{aug} \times \Omega_s, \quad (43)$$

$$\Omega_I^{aug} = \Omega_d^{aug} \times \Omega_p^{aug} \times \Omega_s, \quad (44)$$

with (denoting by F^{-1} the quantile function associated with a cumulative distribution function F)

$$\Omega_d^{aug} = \prod_{i=1}^{n_d} \left[\inf_{d_i \in \Omega_{d_i}} F_{d_i}^{-1}(\alpha), \sup_{d_i \in \Omega_{d_i}} F_{d_i}^{-1}(1 - \alpha) \right], \quad (45)$$

$$\Omega_p^{aug} = \prod_{i=1}^{n_p} \left[F_{p_i}^{-1}(\alpha), F_{p_i}^{-1}(1 - \alpha) \right], \quad (46)$$

$$\Omega_{r_E}^{aug} = \left[F_{r_E}^{-1}(\alpha), F_{r_E}^{-1}(1 - \alpha) \right], \quad (47)$$

$$\Omega_s = \{s^1, \dots, s^{n_s}\}, \quad (48)$$

and α is a degree of confidence chosen by the user (different values of α could be considered for each set of the Cartesian products Ω_d^{aug} , Ω_p^{aug} , and for $\Omega_{r_E}^{aug}$).

The dimensions of Ω_E^{aug} and Ω_I^{aug} are, respectively, equal to $n_d + n_p + 2$ and $n_d + n_p + 1$. We suppose that $n_d + n_p$ is relatively small (less than 12). Under this assumption, the kriging model is particularly well suited to our approach. When using this technique, a metamodel of an expensive function denoted M is built in the form of a Gaussian

stochastic process \tilde{M} whose distribution is characterized by several parameters called hyperparameters. The responses of M over a design of experiments (DoE) are first used to calibrate those hyperparameters. The mean μ , the autocorrelation function and the standard deviation σ of the a posteriori distribution \tilde{M} are then analytically deduced from the hyperparameters and the responses of M at the DoE (Cand and Dupuy 2009). Thus, at each point x of the input space of M , the variable $\tilde{M}(x)$ provides a approximated model in the form of a Gaussian random variable with distribution $\mathcal{N}(\mu(x), \sigma(x)^2)$. The mean $\mu(x)$ is used as predictor while the standard deviation $\sigma(x)$ measures the accuracy of the predictor. This latter information makes kriging metamodel particularly well suited to active learning. Therefore, the metamodel used in AK-ECO is the kriging model since it gives good predictions and provides information about the accuracy of its prediction through the variance of the kriging which will be useful for the enrichment of the models.

We can notice that $\Omega_E^{aug} = \Omega_I^{aug} \times \Omega_{r_E}^{aug}$. Thus, to calibrate the metamodels, we only use one DoE of Ω_E^{aug} . Using one DoE is interesting when the two constraints depend on the same process \mathcal{Y} since each simulation can be used to enrich both metamodels. Indeed, in that case, we recall that to evaluate M_E and M_I at a point (x_d, x_p, x_{r_E}, s^j) , we only need the spectral moments of the process $\mathcal{Y}_1(x_d, x_p, s^j; \cdot)$.

Remark 9 In this paper, the outputs are noise-free therefore the kriging method is adapted. When data noise is considered, the Gaussian Process regression technique (Rasmussen 2004) can be used in AK-ECO.

4.2 Procedure

To solve the reformulated problem (38), AK-ECO begins with the initialization of the design point and the kriging models. Then, the reformulated problem is solved through cycles of optimization. The initialization and the optimization cycle structure are described below.

Initialization: the initial design point d^0 is chosen by the user. An initial DoE, denoted DoE^0 , is computed and used to calibrate the initial metamodels \tilde{M}_E^0 , \tilde{M}_I^0 of the functions M_E and M_I (see Sect. 3.3 for more details). At the end of the initialization, the first cycle of optimization ($k = 1$) can begin.

Optimization cycle: we respectively denote d^{k-1} , DoE^{k-1} , \tilde{M}_E^{k-1} , and \tilde{M}_I^{k-1} , the design point, DoE, and kriging models recovered from the initialization if $k = 1$ or

from the previous cycle if $k > 1$. Each cycle is numbered k and is decomposed into two steps:

Step 1 Local enrichment at d^{k-1} of the metamodels \tilde{M}_E^{k-1} and \tilde{M}_I^{k-1} . For each metamodel:

Step 1.a. An accuracy criterion assesses the precision of the metamodel at d^{k-1} (we detail this step in Sect. 3.4).

Step 1.b. If the metamodel is not accurate enough, one local enrichment is carried out. The local refinement of the metamodel consists in adding to the shared DoE the point x_{enr} selected by the procedure described in Sect. 3.5. The simulator is evaluated at this point and the spectral moments obtained are used to recalibrate all the kriging models.

Steps 1.a and 1.b are repeated until each kriging model meets the accuracy condition of step 1.a. At the end of step 1, the enriched DoE and kriging models are denoted DoE^k , \tilde{M}_E^k , and \tilde{M}_I^k . For each point of the respective augmented spaces, the predictive means of the kriging models are respectively denoted $\mu_E^k(x_d, x_p, x_{r_E}, s^j)$ and $\mu_I^k(x_d, x_p, s^j)$.

Step 2. The reformulated problem (38) is solved using the optimization algorithm chosen by the user starting from d^{k-1} . At each iteration of the optimization, the constraints are estimated with Monte Carlo and the expensive functions are replaced by their current surrogates. For a design d , those estimations, denoted $p_E^k(d)$ and $p_I^k(d)$, are given by:

$$p_E^k(d) = \frac{1}{n_{MC}} \sum_{i=1}^{n_{MC}} F_{\epsilon} \left(\sum_{j=1}^{n_s} \exp \left(\mu_E^k(x_d^i, x_p^i, x_{r_E}^i, s^j) \right) \right), \quad (49)$$

$$p_I^k(d) = \frac{1}{n_{MC}} \sum_{i=1}^{n_{MC}} F_{r_1} \left(\sum_{j=1}^{n_s} T p^j \mu_I^k(x_d^i, x_p^i, s^j) \right), \quad (50)$$

where $\{(x_d^i, x_p^i, x_{r_E}^i), i = 1, \dots, n_{MC}\} = \Omega_{MC}(d)$ is the Monte Carlo sample of the random vector (X_d, X_p, X_{r_E}) . Step 2 does not require any call to the expensive simulator. Once the optimization algorithm has converged, a new design point denoted d^k is obtained.

At the end of each cycle k , the following condition is evaluated:

$$\left\| \overline{d^{k-1}} - \overline{d^k} \right\| < \epsilon_d \quad \text{OR} \quad \left| \overline{\text{cost}(d^{k-1})} - \overline{\text{cost}(d^k)} \right| < \epsilon_{\text{cost}} \quad (\text{stopping condition})$$

where \overline{d} and $\overline{\text{cost}(d)}$ are the normalizations of d and $\text{cost}(d)$ in $[0, 1]$. If this condition is met, AK-ECO is stopped and the minimum retained, denoted d^{\min} , is d^k , otherwise, $k = k + 1$ and a new cycle begins from step 1. The stopping criterion of AK-ECO does not include a condition on the satisfaction of the constraints since this point is verified at the end of the optimization during step 2. The full procedure of AK-ECO is summarized in Fig. 1.

Remark 10 If the random vector X_d depends on d such that $X_d = d + X$ with X a zero-mean random vector, it is possible to use the same Monte Carlo sample Ω_{MC} throughout AK-ECO where $\Omega_{MC} = \{(x^i, x_p^i, x_{r_E}^i), i = 1, \dots, n_{MC}\}$ is a sample of (X, X_p, X_{r_E}) . It follows that $\Omega_{MC}(d) = \{(d + x^i, x_p^i, x_{r_E}^i), (x^i, x_p^i, x_{r_E}^i) \in \Omega_{MC}\}$.

4.3 Kriging models initialization

The goal of the first kriging models is to provide good predictions of their respective functions over the whole augmented spaces. A space-filling DoE is therefore appropriate. As explained above, we use one DoE for both metamodels: only one sample of Ω_E^{aug} is needed. Therefore a space-filling DoE of n_{DoE}^0 points of $\Omega_d^{\text{aug}} \times \Omega_p^{\text{aug}} \times \Omega_{r_E}^{\text{aug}}$ is constructed. We then concatenate to this DoE a uniform sample of n_{DoE}^0 points of Ω_S . The resulting DoE is denoted DoE^0 . The simulator is evaluated for each point of DoE^0 to calibrate the initial kriging models denoted \widetilde{M}_E^0 and \widetilde{M}_I^0 .

4.4 Accuracy criteria

During step 1 of the k -th cycle of optimization, the current kriging model \widetilde{M}_E^{k-1} at (x_d, x_p, x_{r_E}, s^j) follows a normal distribution with mean and standard deviation denoted $\mu_E^{k-1}(x_d, x_p, x_{r_E}, s^j)$ and $\sigma_E^{k-1}(x_d, x_p, x_{r_E}, s^j)$. To evaluate the precision of the approximation $p_E^{k-1}(d)$ of the true failure probability at d , we adapt the approach proposed by Dubourg (2011) and compute the following quantities:

$$p_{E,\pm}^{k-1}(d) = \frac{1}{n_{MC}} \sum_{i=1}^{n_{MC}} F_{\epsilon} \left(\sum_{j=1}^{n_s} \exp \left(\mu_E^{k-1} \left(x_d^i, x_p^i, x_{r_E}^i, s^j \right) \pm 2\sigma_E^{k-1} \left(x_d^i, x_p^i, x_{r_E}^i, s^j \right) \right) \right). \quad (51)$$

As the exponential function and F_{ϵ} are strictly increasing, we have: $p_{E,-}^{k-1}(d) < p_E^{k-1}(d) < p_{E,+}^{k-1}(d)$. The distance between

$p_{E,-}^{k-1}(d)$ and $p_{E,+}^{k-1}(d)$ is an indicator of the uncertainty of the constraint estimation $p_E^{k-1}(d)$. In Dubourg (2011), a criterion based on the ratio between similar optimistic and pessimistic estimations of the failure probability is proposed. However, since it is useless to know precisely the true failure probability if it is far from p_s , we modify this latter criterion. In AK-ECO, the metamodel is considered accurate enough if the following condition is met:

$$\frac{|p_E^{k-1}(d^{k-1}) - p_s|}{p_{E,+}^{k-1}(d^{k-1}) - p_{E,-}^{k-1}(d^{k-1})} > 1. \quad (\text{Criterion E})$$

This criterion is met if the distance between the low and high estimations of the constraint at d^{k-1} is less than the distance between the estimation of the constraint at d^{k-1} and p_s . In this case, we have reasonable grounds to believe that the kriging model accurately predicts whether a point near d^{k-1} belongs or not to the feasible domain.

To avoid a too large number of enrichment steps during the same cycle, a maximal number n_{\max} of enrichment steps are imposed for each metamodel and cycle. Finally, \widetilde{M}_E^{k-1} is considered accurate enough if $p_{E,-}^{k-1}(d^{k-1}) > p_s - \epsilon_p$ and $p_{E,+}^{k-1}(d^{k-1}) < p_s + \epsilon_p$ where ϵ_p is chosen by the user. This last condition indicates that it is not necessary to improve the accuracy of the metamodel beyond a certain threshold defined by ϵ_p and therefore it reduces the number of enrichments required. Hence, \widetilde{M}_E^{k-1} is enriched if Criterion E.b is not met and this criterion is defined as:

$$\text{Criterion E is met OR } (n_E^k \geq n_{\max}) \quad \text{OR} \quad (p_s - \epsilon_p < p_{E,-}^{k-1}(d^{k-1}) < p_{E,+}^{k-1}(d^{k-1}) < p_s + \epsilon_p) \quad (\text{Criterion E.b})$$

For the integral-based constraint, a similar criterion is proposed. We consider the kriging model \widetilde{M}_I^{k-1} whose mean and standard deviation at (x_d, x_p, s^j) are denoted $\mu_I^{k-1}(x_d, x_p, s^j)$ and $\sigma_I^{k-1}(x_d, x_p, s^j)$. The function F_{r_1} is also increasing and $p^j > 0$ for $j = 1, \dots, n_s$. Thus we have, for all d : $p_{I,-}^{k-1}(d) < p_I^{k-1}(d) < p_{I,+}^{k-1}(d)$ with

$$p_{I,\pm}^{k-1}(d) = \frac{1}{n_{MC}} \sum_{i=1}^{n_{MC}} F_{r_1} \left(\sum_{j=1}^{n_s} T p^j \left(\mu_I^{k-1} \left(x_d^i, x_p^i, s^j \right) \pm 2\sigma_I^{k-1} \left(x_d^i, x_p^i, s^j \right) \right) \right). \quad (52)$$

where n_E^k is the number of enrichment steps of the metamodel during cycle k .

The accuracy criterion for the integral-based constraint at d^{k-1} is:

$$\frac{|p_I^{k-1}(d^{k-1}) - p_s|}{p_{I,+}^{k-1}(d^{k-1}) - p_{I,-}^{k-1}(d^{k-1})} > 1. \quad (\text{Criterion I})$$

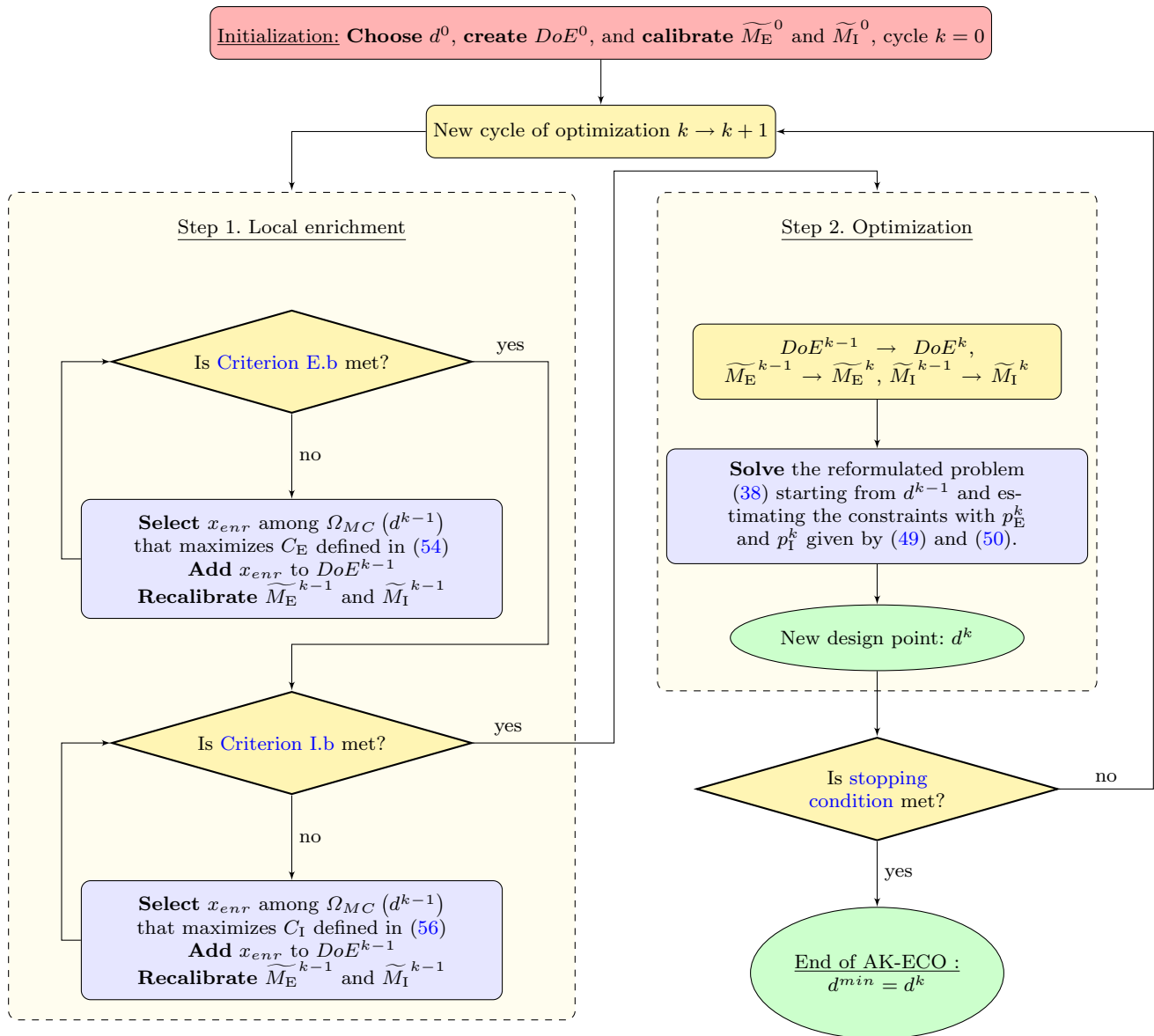


Fig. 1 Flowchart of AK-ECO

The metamodel \widetilde{M}_I^{k-1} is enriched if Criterion I.b is not met and this criterion is defined as:

Criterion I is met OR $(n_I^k \geq n_{\max})$

$$\text{OR } \left(p_s - \epsilon_p < p_{I,-}^{k-1}(d^{k-1}) < p_{I,+}^{k-1}(d^{k-1}) < p_s + \epsilon_p \right) \quad (\text{Criterion I.b})$$

where n_I^k is the number of enrichment steps of the metamodel during cycle k .

Therefore, during each cycle of AK-ECO, the number of enrichments is at most equal to n_{\max} multiplied by the number of metamodels.

When both criteria Criterion E.b and Criterion I.b are met, step 1 ends and step 2 begins.

4.5 Selection of the enrichment point

During the k -th cycle, if Criterion E.b is not met, the model \widetilde{M}_E^{k-1} is not considered sufficiently accurate at d^{k-1} . To improve its precision, a point x_{enr} maximizing a learning function C_E is selected among the Monte Carlo sample $\Omega_{MC}(d^{k-1})$ used in equation (49) to estimate the extreme-based constraint at d^{k-1} . Hence, x_{enr} is given by:

$$x_{enr} = \underset{\Omega_{MC}(d^{k-1}) \times \{s^1, \dots, s^{n_s}\}}{\operatorname{argmax}} C_E(x_{d^{k-1}}^i, x_p^i, x_{r_E}^i, s^j). \quad (53)$$

The goal of criterion C_E is to favour points where the uncertainty of prediction of M_E^{k-1} implies important uncertainties on the constraint estimation at d^{k-1} :

$$\begin{aligned} C_E(x_d^i, x_p^i, x_{r_E}^i, s^j) &= f_{(x_d, x_p, x_{r_E})}(x_d^i, x_p^i, x_{r_E}^i) \\ &\times \left[F_e \left(e^{\mu_E^{k-1}(x_d^i, x_p^i, x_{r_E}^i, s^j)} + 2\sigma_E^{k-1}(x_d^i, x_p^i, x_{r_E}^i, s^j) \right) \right. \\ &+ \sum_{j' \neq j} e^{\mu_E^{k-1}(x_d^i, x_p^i, x_{r_E}^i, s^{j'})} \Big) \\ &- F_e \left(e^{\mu_E^{k-1}(x_d^i, x_p^i, x_{r_E}^i, s^j)} - 2\sigma_E^{k-1}(x_d^i, x_p^i, x_{r_E}^i, s^j) \right) \\ &\left. + \sum_{j' \neq j} e^{\mu_E^{k-1}(x_d^i, x_p^i, x_{r_E}^i, s^{j'})} \right), \end{aligned} \quad (54)$$

with $f_{(x_d, x_p, x_{r_E})}$ the probability density function of the random vector (X_d, X_p, X_{r_E}) . Once x_{enr} is selected, it is added to the current DoE, DoE^{k-1} , and one call to the simulator is made at this point.

For the integral-based constraint, the idea is the same, if Criterion I.b is not met, a new point x_{enr} is selected as follows:

$$x_{enr} = \underset{\Omega_{MC}(d^{k-1}) \times \{s^1, \dots, s^{n_s}\}}{\operatorname{argmax}} C_I(x_{d^{k-1}}^i, x_p^i, s^j), \quad (55)$$

where

$$\begin{aligned} C_I(x_d^i, x_p^i, s^j) &= f_{(x_d, x_p)}(x_d^i, x_p^i) \\ &\times \left[F_{r_1} \left(T p^j \left(\mu_I^{k-1}(x_d^i, x_p^i, s^j) + 2\sigma_I^{k-1}(x_d^i, x_p^i, s^j) \right) \right) \right. \\ &+ \sum_{j' \neq j} T p^{j'} \mu_I^{k-1}(x_d^i, x_p^i, s^{j'}) \Big) \\ &- F_{r_1} \left(T p^j \left(\mu_I^{k-1}(x_d^i, x_p^i, s^j) - 2\sigma_I^{k-1}(x_d^i, x_p^i, s^j) \right) \right) \\ &\left. + \sum_{j' \neq j} T p^{j'} \mu_I^{k-1}(x_d^i, x_p^i, s^{j'}) \right). \end{aligned} \quad (56)$$

Remark 11 Usually in reliability analysis, adaptive strategies aim at improving a metamodel near the limit state surface of the considered performance function (Teixeira et al. 2021; Moustapha et al. 2022). The learning functions proposed in this paper do not pursue the same goal since in our reformulated problem, each constraint involves an expectation and not a failure probability. Our approach is closer to the enrichment of the metamodel seeking to reduce the variance of an expectation of the form $\mathbb{E}_X[\tilde{M}(X)]$ where X is a random vari-

able et \tilde{M} is a kriging model as proposed in Huchet et al. (2019).

In our case, the expectations involved in the reformulated constraints can be written as follows:

$$\mathbb{E}_X \left[F \left(\sum_{j=1}^{n_s} H(\tilde{M}(X, s^j)) \right) \right] \quad (57)$$

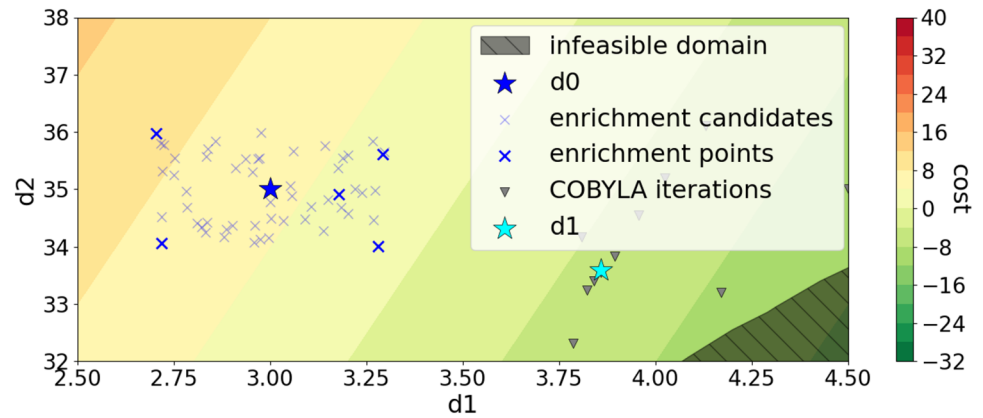
where F and H are two monotonic functions. The variance of this quantity with respect to the kriging distribution of \tilde{M} is difficult to estimate. At each point x of the Monte Carlo sample of X used to approximate the expectation in (57), our learning functions therefore simply consider the uncertainty of $F \left(\sum_{j=1}^{n_s} H(\tilde{M}(x, s^j)) \right)$ from the standard deviation of $\tilde{M}(x, s^j)$.

4.6 Visualization of one cycle of AK-ECO

To illustrate one cycle of AK-ECO, we consider the minimization of a cost function in a two-dimensional design space with extreme-based and integral-based constraints. The level sets of the cost function that we want to minimize are displayed in Fig. 2. The infeasible domain is the black hatched area. After initialization of the metamodels, the first cycle of AK-ECO begins by evaluating their accuracy at the initial design point d^0 (step 1.a). Since they are not accurate enough, enrichment candidates of the augmented space are considered (projections in the design space of several candidates are represented with light blue crosses). Enrichment points are then selected among these candidates until the precision criteria are met (step 1.b). The projection of 5 of these points are indicated by thick blue crosses in the Fig. 2. Once the accuracy criteria are met, step 2 begins and the optimization problem is solved with an optimization algorithm using the enriched metamodels. The iterations of this optimization are represented by grey triangles. This resolution provides a new design point d_1 which will be the starting point of the next cycle of AK-ECO.

5 Application to the harmonic oscillator problem introduced in Sect. 2.4

To validate the method proposed in the previous section, we study the resolution of the reformulated problem of the piece-wise stationary harmonic oscillator described in Sect. 2.4. First, a resolution of the problem with a double-loop approach using the Monte Carlo method to estimate the constraints is used as a reference. Then, the problem is

Fig. 2 Visualization of the first cycle of AK-ECO**Table 1** Parameters of the problem

Parameter	ρ	n_T	ΔT	T	n_s	p_s
Value	1	100	216	21600	7	10^{-4}

solved with AK-ECO. These two methods solve the reformulated problem with constraints involving expectations. The resolution of this problem with a probabilistic formulation of the constraints (see Sect. 3) is carried out with our implementation of RIA, PMA, SORA and the Stiang approach presented in the introduction section.

5.1 Cost function, sources of uncertainties and parameters of the problem

Here the cost function is:

$$\text{cost}(d_1, d_2) = d_2 - 10d_1. \quad (58)$$

The optimization problem is solved on the design space $\Omega_d = [1, 5] \times [20, 50]$ and for the parameters ρ , n_T , ΔT , T , n_s and p_s given in Table 1.

The distributions considered for the random variables X_{d_1} , X_{d_2} , X_p , X_{r_1} , X_{r_2} and X_{r_3} are given in Table 2 and the couples (s^j, p^j) , $j = 1, \dots, 7$ in Table 3.

The notations $\mathcal{U}[a, b]$ and $\mathcal{N}(\mu, \sigma^2)$ refer, respectively, to the uniform distribution on $[a, b]$ and the normal distribution of mean μ and standard deviation σ .

Here, the functions involved in the constraints are actually not very expensive and massive Monte Carlo simulations with samples of size 30000 can be carried out. So we are able to check the performances of the different optimization methods. The level sets of the cost function and of the logarithm of the three constraints are displayed in Fig. 3. In Fig. 3, the black dotted lines correspond to the design points where each failure probability equals p_s and the estimation of the i -th failure probability with Monte Carlo is denoted pi ($i = 1, 2, 3$) in the legend.

Table 2 Distributions of X_{d_1} , X_{d_2} , X_p , X_{r_1} , X_{r_2} , X_{r_3}

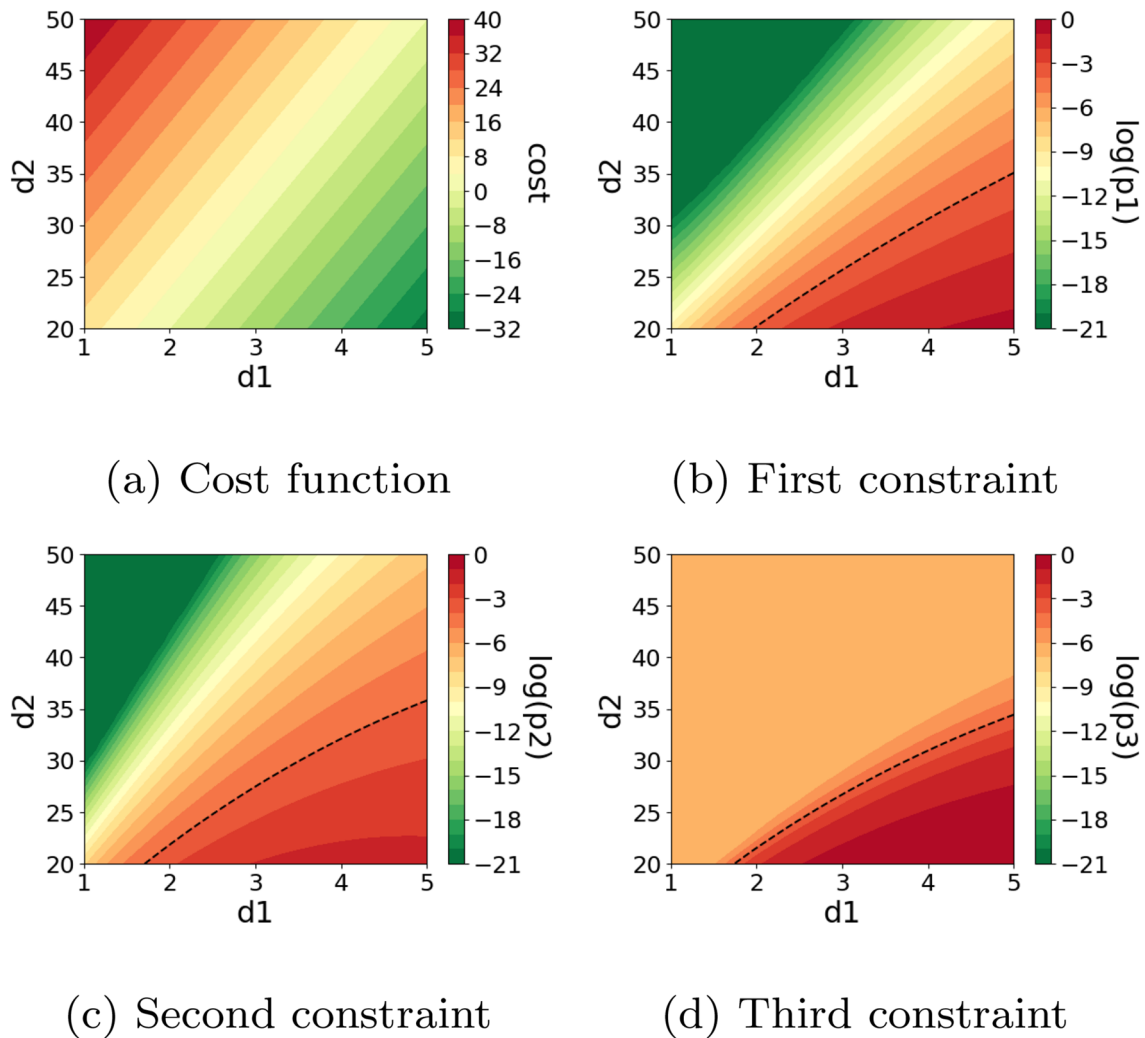
Uncertainty	Distribution
X_{d_1}	$\mathcal{U}[d_1 - 0.3, d_1 + 0.3]$
X_{d_2}	$\mathcal{U}[d_2 - 1, d_2 + 1]$
X_p	$\mathcal{U}[0.5, 1.5]$
X_{r_1}	$\mathcal{N}(1, 0.1^2)$
X_{r_2}	$\mathcal{N}(2.5, 0.25^2)$
X_{r_3}	$\mathcal{N}(15, 3^2)$

5.2 Implementations

The reference results are obtained using the COBYLA (Powell 1994) optimization algorithm (which is a trust-region method performing linear approximations to the objective and constraint functions) and a massive Monte Carlo method to estimate the failure probabilities (this approach is denoted MC). The COBYLA algorithm is also used for the other methods. The FORM method in RIA is performed with the Abdo-Rackwitz algorithm (Abdo and Rackwitz 1991) available in the python package OpenTURNS (Baudin et al. 2016). The HMV algorithm (Youn et al. 2003) is implemented to solve the inverse reliability analysis in PMA. In SORA and Stiang, the SQP (Nocedal and Wright 2006) algorithm is chosen instead of HMV since it performs better on the studied case. For AK-ECO, the initial space-filling DoE is a Latin Hypercube Sampling (LHS) maximin (McKay et al. (2000); Santner et al. 2018) of size 50. The maximum number of enrichment steps per cycle and per constraint n_{max} is set to 15. The size n_{MC} of the sample used in the MC method is 30000. For Stiang, SORA and

Table 3 Couples (s^j, p^j)

j	1	2	3	4	5	6	7
s^j	1.20	1.16	1.10	1.05	0.99	0.95	0.90
p^j	0.21	0.17	0.18	0.16	0.13	0.09	0.06

**Fig. 3** Level sets of the cost function and of the logarithm of the failure probabilities appearing in each constraint

AK-ECO, the cycles of optimization stop if the stopping condition introduced in Sect. 3.2 is met for ϵ_d and ϵ_{cost} equal to 10^{-3} . In Stieng and AK-ECO, the kriging implementation of OpenTURNS is used with a constant trend and a 3/2-Matérn covariance kernel. In AK-ECO, the states s_j are treated as continuous variables by the kriging kernel since, in the oscillator application, the $s^j, j = 1, \dots, n_s$ are real numbers. In Stieng, the initial DoE is a Sobol sequence (Sobol' 1967) of size 12. A Sobol sequence of size 40 is used for the second cycle, 160 for the third one and 400 for the next cycles. In this paper, the DoEs are always normalized to calibrate the kriging models.

5.3 Numerical results

The problem under study is solved with each approach starting from the centre (3, 35) of the design space. The results are displayed in Table 4. The first and second rows indicate the design point d^{min} obtained by each approach and the value of the cost function at this point. For $i = 1, 2, 3$, the i -th failure probability at d^{min} is then estimated with a massive Monte Carlo of 30000 points and the result is denoted $p_i^{MC}(d^{min})$. Finally, as explained in remark 6, the expensive part of the constraints is the evaluation of the spectral moments of $\mathcal{D}_1(x_d, x_p, s^j; \cdot)$. Therefore, during the resolution

of the problem, one estimation of the spectral moments for one point (x_d, x_p, s^j) is considered as one call to the expensive simulator. The number of calls to the simulator by each method is denoted n_{call} . It is important to notice that, unlike usual papers in reliability analysis, the number n_{call} does not refer to the number of calls to the performance functions but to the number of simulations. Hence, for RIA, PMA, SORA and Stiang, the number of calls to the performance functions is equal to $n_{call}/7$ since $n_s = 7$.

We observe that all the methods converge towards the same design point. However, AK-ECO provides the closest design point to the reference point obtained with MC and requires far fewer calls to the expensive simulator than the comparison methods: only 252 calls are required (50 for the initial DoE and 202 for local enrichments of the metamodels during the optimization cycles). This is due to the fact that AK-ECO is well adapted to the reformulated problem: each call to the simulator allows to enrich every kriging model and the simulation is performed only at the relevant states s^j . Furthermore, among the compared methods only RIA and AK-ECO provide an estimation of the failure probabilities. At the design point obtained with RIA, the first, second and third failure probabilities are estimated with FORM as 1.1×10^{-4} , 1.3×10^{-4} , 0.8×10^{-4} . The probabilities estimated with AK-ECO at the design point obtained with this algorithm are 0.7×10^{-4} , 1.0×10^{-4} , 0.1×10^{-4} . Hence, with AK-ECO, we observe a good approximation of the failure probabilities since they are close to the reference probabilities obtained in the column MC.

For SORA, the Stiang approach and AK-ECO, at the end of cycle k a design point d^k is obtained. The evolution of $\log \left(\left| \overline{cost(d^{k-1})} - \overline{cost(d^k)} \right| \right)$ for each method and each cycle k is displayed in Fig. 4a and the evolution of $\log \left(\left\| \bar{d}^k - \bar{d}^{k-1} \right\| \right)$ in Fig. 4b where $cost(d^{k-1})$ and \bar{d}^k refer, respectively, to the normalization of $cost(d^k)$ function and of d^k in $[0, 1]$.

We observe that the resolution of the studied problem takes 5 cycles for AK-ECO to converge while 7 and 20 cycles are necessary for SORA and Stiang to meet the stopping condition. In AK-ECO, the closer the design

point is to the true infeasible domain boundary, the more enrichment steps are performed. During the first cycle, 22 points are added to the DoE while 45 enrichment steps are performed during the second, third and last ones.

Moreover, the failure probabilities p_1^{MC} , p_2^{MC} , p_3^{MC} have been evaluated with a Monte Carlo of 30000 points at the design point obtained at the end of each cycle of SORA, Stiang and AK-ECO and their evolution is displayed in Fig. 5. We can see that with Stiang and AK-ECO, the true constraints are satisfied at the end of each cycle while it takes 4 cycles for SORA (actually, with AK-ECO, p_2^{MC} is slightly above the threshold 10^{-4} at the end of the third cycle).

The resolution of the problem has also been repeated with AK-ECO from 20 different starting design points selected with a LHS maximin of the design space. Each time, the initial kriging models are calibrated with a new DoE. The results show that the performance of AK-ECO is not affected by the initial DoE or the initial design point since the algorithm converges towards the good design point each time and with a number of simulations varying from 174 to 416 with a mean number of calls equal to 229.1.

6 Application to a second harmonic oscillator problem

In this section we solve another oscillator problem to show how AK-ECO performs when the number of states n_s increases compared to the other methods.

6.1 Second oscillator problem and reformulation

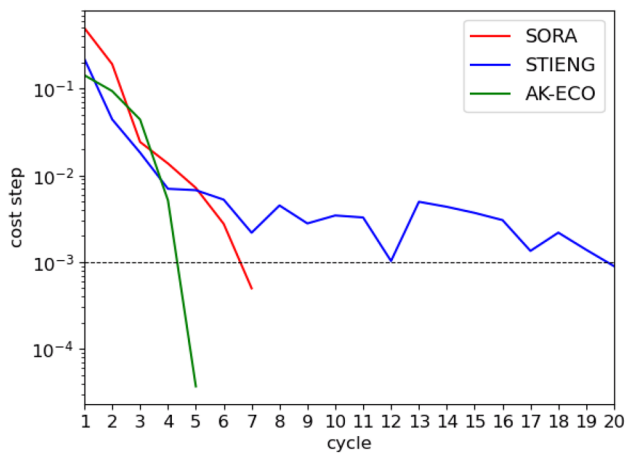
We consider in this section the following problem:

$$\begin{aligned} \min_{d \in \Omega_d} cost(d) \quad \text{such that} \\ \mathbb{P}_{X_d, X_p, \eta} \left(\max_{t \in [0, T]} \mathcal{D}(X_d, X_p; t) > r_1 \right) &< p_s \\ \mathbb{P}_{X_d, X_p, X_{r_2}, \eta} \left(\int_0^T \left(|\mathcal{D}''(X_d, X_p; t)| - \rho \right)^+ dt > X_{r_2} \right) &< p_s \end{aligned} \quad (59)$$

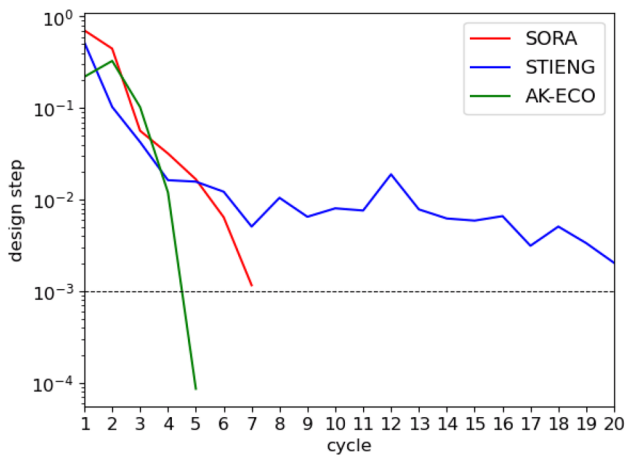
where the random processes \mathcal{D} , \mathcal{D}'' , and η , the design space Ω_d , the random vectors X_d and X_p , and the values of T and

Table 4 Results of AK-ECO and the comparison methods for the harmonic oscillator problem

	MC	RIA	PMA	SORA	Stiang	AK-ECO
d^{min}	(5.0, 35.74)	(5.0, 35.22)	(5.0, 35.04)	(5.0, 36.77)	(5.0, 37.29)	(5.0, 35.73)
$cost(d^{min})$	- 14.26	- 14.78	- 14.96	- 13.23	- 12.70	- 14.27
$p_1^{MC}(d^{min})$	0.8×10^{-4}	1.0×10^{-4}	1.0×10^{-4}	0.4×10^{-4}	0.3×10^{-4}	0.8×10^{-4}
$p_2^{MC}(d^{min})$	1.0×10^{-4}	1.3×10^{-4}	1.3×10^{-4}	0.6×10^{-4}	0.5×10^{-4}	1.0×10^{-4}
$p_3^{MC}(d^{min})$	0.1×10^{-4}	0.8×10^{-4}	0.4×10^{-4}	0	0	0.1×10^{-4}
n_{call}	3.57×10^6	791175	29393	15722	53200	252



(a) Evolution of $\log \left(\left| \overline{\text{cost}}(d^{k-1}) - \overline{\text{cost}}(d^k) \right| \right)$



(b) Evolution of $\log \left(\left\| \overline{d^k} - \overline{d^{k-1}} \right\| \right)$

Fig. 4 Evolution of the stopping condition for SORA, StienG and AK-ECO

ρ are the same as the ones used in the previous oscillator problem. They are defined in Sect. 2.4 and Sect. 4.

In problem (59), the *cost* function is defined as follows:

$$\text{cost}(d_1, d_2) = \exp \left(\frac{(d_1 - 3)^2}{10} + \frac{(d_2 - 20)^2}{1000} \right). \quad (60)$$

Moreover, we consider $p_s = 10^{-3}$, $r_1 = 0.3$, $X_{r_2} \sim \mathcal{N}(20, 5^2)$, and the states are defined in Table 5.

Using the same reasoning as for the oscillator problem described in Sect. 2.4, problem (59) can be reformulated as an optimization problem with constraints involving one extreme-based and one integral-based reformulated failure probability, as in problem (38).

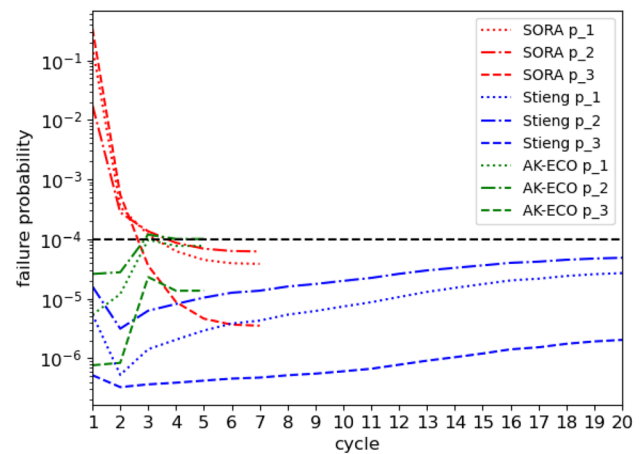


Fig. 5 Evolution of the Monte Carlo estimation of the failure probabilities for SORA, StienG and AK-ECO

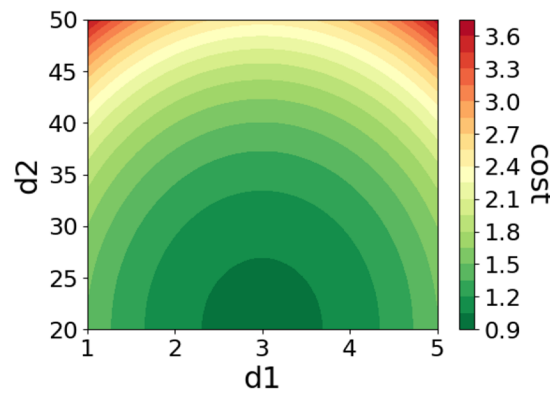
These reformulated constraints are evaluated by Monte Carlo with a sample of 3000 points to obtain the level sets displayed in Fig. 6. The black dotted lines correspond to the design points where each failure probability equals p_s and the estimation of the i -th failure probability with Monte Carlo is denoted p_i ($i = 1, 2$) in the legend. The level sets of the cost function are displayed as well in the Fig. 6.

6.2 Implementations

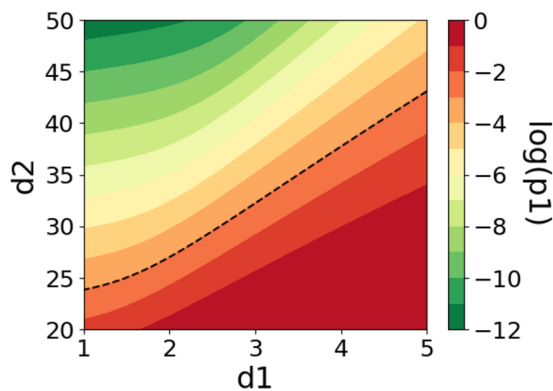
As for the first oscillator problem, the optimizer used for every method is COBYLA. The reference results are obtained using Monte Carlo to estimate the reformulated constraints. The configurations of RIA, PMA, SORA, StienG and AK-ECO are the same as those detailed in Sect. 4.2 except for the Monte Carlo sample size. Indeed, since the probability threshold is $p_s = 10^{-3}$, the Monte Carlo sample size for the reference method and for AK-ECO is 3000. Moreover, the initial DoE of AK-ECO is now composed of 30 points. In StienG, the initial DoE is a Sobol sequence of size 9, a Sobol sequence of size 30 is used for the second cycle, 90 for the third one and 300 for the next cycles.

Table 5 States of the second oscillator problem

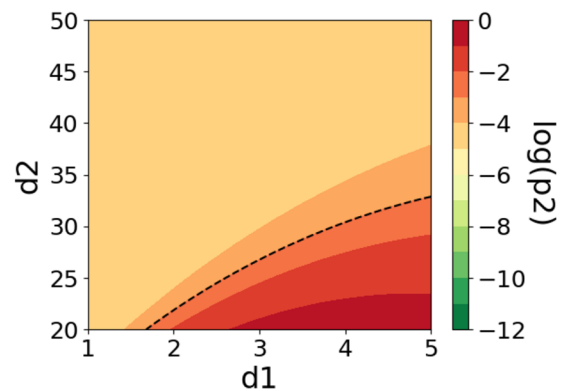
n_s	s^j for $j = 1, \dots, 50$	p^j for $j = 1, \dots, 50$
50	$1.4 - (j - 1) \frac{1.4 - 0.8}{n_s - 1}$	$\frac{1}{j}$
		$\sum_{i=1}^{50} \frac{1}{i}$



(a) Cost function



(b) First constraint



(c) Second constraint

Fig. 6 Level sets of the cost function and of the logarithm of the failure probabilities appearing in each constraint

6.3 Numerical Results

The reformulated problem studied in this section is solved starting from the centre point (3, 35) of the design space with every approach. The results are displayed in Table 6. We use the same notations for Table 4 and Table 6 except that p_i^{MC} ($i = 1, 2$) are computed with a Monte Carlo of 3000 points.

We observe in Table 6 that all methods converge towards the same point even if the constraints are not well estimated by each approach. Moreover, AK-ECO requires far fewer expensive function calls than the comparison methods. Indeed, contrary to the other methods, AK-ECO is not sensitive to the number of states n_s and therefore it performs much better in terms of n_{call} when n_s increases compared to the alternatives. Finally, the first constraint in d^{min} is over-estimated with AK-ECO. To improve this estimation, it is possible to change the parameters of the accuracy criteria

discussed in Sect. 3.4, for example, by increasing the maximum number of enrichments per cycle (we used the same parameters for each problem presented in this paper).

7 Application to the floating offshore wind turbine problem

We now consider a modified version of the floating offshore wind turbine described in Robertson et al. (2014): the wind turbine is equipped with a semi-submersible floater connected to the seabed by three mooring lines (see Fig. 7). In this section, we aim at minimizing the material cost of the mooring lines while considering reliability constraints. The mooring system must limit the floater movements to ensure the turbine production, avoid compression in the mooring lines and withstand the damage caused by fatigue. The resulting constraints inherit the randomness of the

Table 6 Results of AK-ECO and the comparison methods for the harmonic oscillator problem 2

	MC	RIA	PMA	SORA	Stieng	AK-ECO
d^{min}	(2.50, 29.51)	(2.46, 29.60)	(2.46, 29.60)	(2.46, 29.57)	(2.52, 29.60)	(2.49, 29.57)
$cost(d^{min})$	1.123	1.129	1.129	1.128	1.122	1.125
$p_1^{MC}(d^{min})$	1.00×10^{-3}	0.80×10^{-3}	0.80×10^{-3}	0.81×10^{-3}	1.04×10^{-3}	0.93×10^{-3}
$p_2^{MC}(d^{min})$	0.04×10^{-3}	0.04×10^{-3}	0.04×10^{-3}	0.04×10^{-3}	0.04×10^{-3}	0.04×10^{-3}
n_{call}	6×10^6	725950	483050	56750	13850	122

marine conditions, the material properties and the model parameters.

7.1 Design variables and design space

The material cost of the mooring system and the constraints depend on three design variables: the length d_1 of the mooring line that can be added to, or deducted from, the nominal mooring length of 841.56m (its domain is $[-0.5, 2]$ (in m)), the mass per unit length $d_2 \in [70, 180]$ (in kg/m), the position d_3 of the connection of the lines to the side columns of the floater (taking values between 0 and 1 which, respectively, correspond to the connection at the bottom and at the top of the columns). We denote $d = (d_1, d_2, d_3)$ and the design space $\Omega_d = [-0.5, 2] \times [70, 180] \times [0, 1]$.

7.2 Definition of the time-dependent processes involved in the constraints

The movements of the structure are determined from the environmental loads occurring during the considered period $[0, T]$ (T is equal to one year) and in particular loadings induced by waves.

The swell is modelled as a succession of waves meeting the structure and defined by their height at any time at a given point. To account for all the possible sea states, we discretize the interval of time $[0, T]$ into n_T subintervals I_i ,

$i = 1, \dots, n_T$, of length ΔT ($\Delta T = 3$ hours). For each interval I_i , the sea elevation is represented by a zero-mean stationary Gaussian random process defined by its spectral density. In this study, we consider the JONSWAP spectral density (Hasselmann et al. 1980) which is characterized by three long-term parameters (the significant wave height, the peak period and the mean wind speed) grouped in s_i which will be called the sea state. The sea elevation process on I_i is denoted $\eta_i(s_i; \cdot)$. We consider that $\eta_i(s_i; \cdot)$ and $\eta_j(s_j; \cdot)$ are independent processes for $i \neq j$. We assume that there are only 7 possible sea states s^1, \dots, s^7 (i.e. $\forall s_i, i = 1, \dots, n_T, s_i \in \{s^1, \dots, s^7\}$). Moreover, we consider only constant wind forces (thrust on Rotor-Nacelle-Assembly and turbine torque) applied on the structure for each sea state.

At the end of the optimization problem, the chosen design variables must restrict the platform movements: the horizontal shifting of the structure (called surge) must be less than a conservative threshold \mathcal{S}_{\max} of 5% of the water depth. Tension in the lines must stay positive and the accumulated fatigue damage in the line must remain below a resistance threshold R . We consider only the tension and the fatigue at the top of each line.

For a fixed sea state s_i , the movements of the platform and the lines are solutions of a linearized equation of motion in which the forces come from environmental loads. The surge and tension at the top of the line $l, l \in \{1, 2, 3\}$, can be written as:

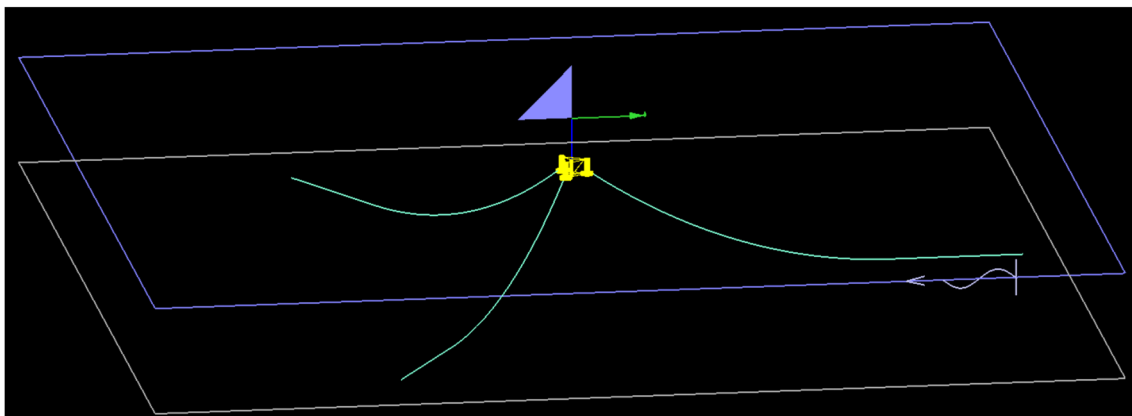


Fig. 7 Perspective view of the floating offshore wind turbine model in Deeplines™

$$\mathcal{S}_i(t) = \mu_{\mathcal{S}_i} + \bar{\mathcal{S}}_i(t), \quad \mathcal{T}_i(t) = \mu_{\mathcal{T}_i} + \bar{\mathcal{T}}_i(t), \quad (61)$$

where $\mu_{\mathcal{S}_i}$ and $\mu_{\mathcal{T}_i}$ are constants obtained computing the static equilibrium. Moreover, $\bar{\mathcal{S}}_i$ and $\bar{\mathcal{T}}_i$ are outputs of linear filters with the sea elevation $\eta_i(s_i; \cdot)$ as input. Taking into account the different sea states, the surge and the tension at the top of the line l , $l \in \{1, 2, 3\}$, on $[0, T]$, denoted, respectively, \mathcal{S} and \mathcal{T} , are defined as follows:

$$\mathcal{S}(t) = \sum_{i=1}^{n_T} \mathcal{S}_i(t) \mathbb{1}_{I_i}(t), \quad \mathcal{T}(t) = \sum_{i=1}^{n_T} \mathcal{T}_i(t) \mathbb{1}_{I_i}(t). \quad (62)$$

We deduce from these definitions and the properties of the sea elevation process that the surge and tension processes are piece-wise stationary Gaussian processes.

We can represent the instantaneous damage occurring at the top of the l -th mooring line, $l \in \{1, 2, 3\}$, as follows:

$$\mathcal{D}^l(t) = \sum_{i=1}^{n_T} \mathcal{D}_i^l(t) \mathbb{1}_{I_i}(t), \quad \forall t \in [0, T], \quad (63)$$

where $\mathcal{D}_i^l(t)$ is the instantaneous damage caused by $\mathcal{T}_i^l(t)$. The accumulated damage over $[0, T]$, also called fatigue, is defined as the integral $\int_0^T \mathcal{D}^l(t) dt$. The distributions of the surge process, the tension processes and the fatigue depend on the design variables d and on model parameters denoted x_{p_1} , x_{p_2} , and x_{p_3} (as well as on a parameter x_{d_2} for the fatigue) which are presented below.

7.3 Model and fatigue threshold uncertainties

To account for the lack of knowledge on certain parameters, uncertainties are considered on the following:

- the wave heading which is represented by a random variable X_{p_1} uniformly distributed between plus and minus 10° around the wind turbine axis;
- two quadratic viscous drag coefficients for the surge and the pitch of the floater, denoted X_{p_2} and X_{p_3} , to account for the approximation of the fitting from decay tests (Burmester et al. 2020). Each of these random variables follows a uniform law, respectively, on $[10^5, 10^6]$ (in $\text{N.s}^2.\text{m}^{-2}$) and $[3 \times 10^{10}, 7 \times 10^{10}]$ (in $\text{N.m.s}^2.\text{rad}^{-2}$);
- the y-intercept of the fatigue law X_{d_2} accounting for experimental scattering. It follows a log-normal distribution with parameters, chosen after the Stiff's fatigue curve for chain, $\sigma_{d_2} = 0.8$ and μ_{d_2} which depends on the mass per unit length d_2 via a linear relation of the Breaking Load (see Rossi (2005) for the fatigue law relation);
- the threshold resistance R for approximation of time-independent Palmer Miner damage approach. It is a log-

normal distribution of parameters $\mu_R = 1$ and $\sigma_R = 0.3$ (Leira et al. 2005).

All of these variables are independent and X_p denotes the random vector $X_p = (X_{p_1}, X_{p_2}, X_{p_3})$.

7.4 Optimization problem formulation

Taking into account all the sources of uncertainty, we consider the following optimization problem:

$$\begin{aligned} \min_{d \in \Omega_d} \text{cost}(d) \quad \text{such that} \\ \mathbb{P} \left(\max_{[0, T]} \mathcal{S}(d, X_p; t) > \mathcal{S}_{\max} \right) &< 10^{-4} \\ \mathbb{P} \left(\min_{[0, T]} \mathcal{T}^l(d, X_p; t) < 0 \right) &< 10^{-4}, \quad l = 1, 2, 3 \\ \mathbb{P} \left(\int_0^T \mathcal{D}^l(d, X_p, X_{d_2}; t) dt > R \right) &< 10^{-4}, \quad l = 1, 2, 3. \end{aligned} \quad (64)$$

The threshold probability of 10^{-4} is recommended by international standards for mooring lines (Veritas 2013) and the cost function is cheap to evaluate. We notice that the surge and tension constraints are extreme-based constraints while the fatigue constraints are integral-based. Besides, since the surge and tension processes are piece-wise stationary Gaussian processes, we can reformulate the problem as described in Sect. 2. We thus obtain a reformulated problem which can be solved with AK-ECO.

Remark 12 Another formulation of the problem studied in this section could have been considered. Indeed, instead of solving an optimization problem with probabilistic constraints, it is also possible to minimize the total expected cost which takes into account the cost of the mooring lines and the costs of failures weighted by their probabilities of occurrence (Kanda 2021; Kroetz et al. 2020). However, although from an economical standpoint the total expected cost is interesting, this formulation has not been chosen here because the costs of failures are often confidential and difficult to estimate, but more importantly, the standards (Veritas 2013) impose to consider constraints as formulated in problem (64).

7.5 Resolution of the reformulated problem

We now solve the reformulated version of the floating offshore wind turbine problem. For given design variables d , parameters x_p and sea state s^j , the means and the spectral moments of the surge and the tension processes are all outputs of a single simulation and are computed with the frequency domain solver of the DeeplinesTM software (Le Cunff et al. 2008) dedicated to offshore engineering applications.

This software is based on the finite elements method and the computational time of one simulation (about 1 minute) is too high to apply naive approaches such as a brut Monte Carlo. The reformulated problem is thus solved with four methods: AK-ECO, SORA, Stiang and a method denoted MC+K1600 which provides the reference results. Since it would be too expensive to evaluate the reformulated constraints with Monte Carlo, in MC+K1600, the expensive functions are replaced by kriging models built from a LHS of 1600 points. The Monte Carlo method is then used with these kriging models to estimate the constraints during the resolution of the optimization problem. For SORA and Stiang, we solve the probabilistic formulation of the problem (see Sect. 3).

The optimization algorithm used for each approach is the COBYLA algorithm. In SORA and Stiang, the SQP algorithm is chosen to solve the inverse reliability analyses. For AK-ECO, the initial DoE is a LHS maximin of size 60. Moreover, a work has been done, but will not be presented in this paper, to reduce the dimension of the variables s^j from 3 to 1. Thus the metamodels of AK-ECO are actually built in a 7-dimensional space. The maximum number of enrichment steps per cycle and per constraint n_{max} is set to 15. For Stiang, SORA and AK-ECO, the cycles of optimization stop if the stopping condition introduced in Sect. 3.2 is met for ϵ_d and ϵ_{cost} equal to 10^{-3} . For AK-ECO, MC+K1600 and Stiang, a kriging with constant trend and 3/2-Matérn covariance kernel is used for every metamodel. A Sobol sequence of 30 points is used to calibrate the kriging models of the first cycle of Stiang. For the second cycle, the size of the sequence is 90 and 300 for the next ones. The same Monte Carlo sample of X_p of size 30000 is used in MC+K1600 and AK-ECO to estimate the reformulated failure probabilities.

7.6 Numerical results

The results obtained by each approach, considering an initial design point at the centre of the design space (0.75, 125, 0.5), are given in Table 7. The design point obtained by each method is denoted d^{min} and $cost(d^{min})$ is

the cost function evaluated at this point normalized between [0, 1] (this normalization is possible since the optima of the *cost* function are known here). The surge, tension and fatigue failure probabilities at d^{min} obtained by each method have been evaluated with Monte Carlo and the kriging models of the MC+K1600 method. The results are denoted $p_S^{K1600}(d^{min})$, $p_T^{K1600}(d^{min})$ and $p_{D^3}^{K1600}(d^{min})$ ($l = 1, 2, 3$). Finally, the number of simulations performed during the resolution of the studied problem with each method is denoted n_{call} .

We observe that each method provides a reliable optimum. However, the design proposed by AK-ECO is much closer to the reference result obtained with MC+K1600 than the ones proposed by SORA and Stiang. This difference is due to the inverse reliability analyses performed during these methods which underestimate the reliability associated with the last constraint. This leads to a sub-optimal design point provided by these approaches. Furthermore, AK-ECO requires much less evaluations of the simulator since only 305 calls were needed (60 for the initial DoE and 245 for the enrichment procedure during the optimization cycles).

8 Conclusion

We have considered in this paper a time-dependent RBDO problem with two types of constraints which involve the maximum and the integral function of a time-dependent stationary or piece-wise stationary Gaussian random process. This kind of problems is inspired by applications that arise in offshore wind turbine design where the movements of a structure are time-dependent stochastic processes whose properties can be derived from input processes representing the marine conditions (i.e. the wind speed and the sea elevation).

To solve this problem efficiently, we have proposed a two-step procedure. First, we use limit theorems to reformulate the constraints into easier to evaluate constraints that are time-independent and depend only on uncertainties represented by random vectors. The extreme value

Table 7 Results of AK-ECO and the comparison methods for the wind turbine problem

	MC+K1600	SORA	Stiang	AK-ECO
d^{min}	(0.862, 108.86, 0)	(2, 141.22, 0)	(2, 140.58, 0)	(0.947, 109.52, 0)
$cost(d^{min})$	0.2818	0.5883	0.5819	0.2867
$p_S^{K1600}(d^{min})$	1.0×10^{-4}	0	0	0.9×10^{-4}
$p_T^{K1600}(d^{min})$ ($l = 1, 2, 3$)	0	0	0	0
$p_{D^3}^{K1600}(d^{min})$ ($l = 1, 2$)	0	0	0	0
$p_{D^3}^{K1600}(d^{min})$	1.0×10^{-4}	0.2×10^{-4}	0.2×10^{-4}	0.9×10^{-4}
n_{call}	1600	16394	5754	305

theory enables us to approximate the extreme-based failure probability while the ergodicity of the process appearing in the integral-based constraint is used to reformulate it. Therefore, we obtain a RBDO problem with constraints involving expectations instead of failure probabilities.

A sum of n_s terms appears in each expectation constraint (where n_s is the number of different stationary distributions involved in the piece-wise stationary process) and one call to an expensive simulator is required to compute each of these terms. We thus propose a new method based on adaptive kriging and called AK-ECO that solves the reformulated problem much faster than the approaches in the literature. In the usual approaches, for each constraint, a metamodel is built to replace the performance function and one evaluation of the performance function leads to n_s simulations. In AK-ECO, the metamodel replaces the expensive function involved in the sum. Thus, one enrichment of the metamodel only requires one simulation. The number of calls to the expensive simulator is dramatically reduced especially when n_s is large as in the offshore wind turbine application.

To illustrate the procedure, two problems involving a harmonic oscillator are introduced. We apply the reformulation and then, we solve the obtained problems with AK-ECO and state-of-the-art algorithms in RBDO. The results show that AK-ECO is better suited than the presented competing approaches for the type of problems considered in our paper. The two-step procedure is then applied to minimize the material cost of a mooring system of a floating offshore wind turbine under extreme- and integral-based constraints. A reliable optimum is thus obtained with few calls to the expensive simulator.

The AK-ECO efficiency relies on the assumptions that the cost function is fast to evaluate and that the dimension of the augmented space is small (say, less than 12). In high dimension, kriging models perform poorly and additional work would be necessary to adapt AK-ECO. In addition, when n_s becomes large, the estimation of the failure probabilities with Monte Carlo as well as the selection of enrichment points can become cumbersome. Hence, AK-ECO would benefit from being coupled with a variance reduction technique. Furthermore, it is assumed that the initial DoE quality is good enough to capture the shape of the feasible domain since the metamodels are only enriched locally during AK-ECO. To improve the quality of the initial DoE, it would be interesting to implement a procedure before starting AK-ECO that enriches the DoE so that the failure probabilities are accurately estimated over the entire design space, which would ensure a good estimation of the feasible domain.

Finally, AK-ECO has been implemented to be coupled with a local optimization algorithm and thus provides a local optimum. To obtain a global optimum, it is possible

to perform multistart optimization with AK-ECO from several initial design points. If one wishes to couple AK-ECO with a global optimizer, it will be necessary to adapt the AK-ECO enrichment strategy. Indeed, the approach proposed in the paper only performs local enrichments of the metamodels in order to obtain a good approximation of the constraints near the current design point at each iteration of the local optimizer. Using a global optimizer implies that the user must determine at each iteration where the local enrichments of the metamodels should be performed (i.e. where the constraints should be known with accuracy over the entire design space).

Appendix of section 1

Extreme-based failure probability reformulation error

Bounds can be obtained on the approximation (15) using the theorem 2.2 of Kratz and Rootzén (1997). We present here the theorem for a process ξ satisfying the conditions of theorem 1 and we show how it can be applied to control the reformulation error.

Rate of convergence of theorem 1

Theorem 2 (Theorem 2.2 of Kratz and Rootzén 1997) *Let ξ be the process introduced in theorem 1 satisfying condition (9) and the following conditions:*

$$\mathbb{E}[(\xi'(t) - \xi'(0))]^2 = 2(k''_{\xi}(\tau) - k''_{\xi}(0)) \leq c\tau^2, \quad \tau \geq 0, \quad (65)$$

$$|k_{\xi}(\tau)| \leq Ct^{-\alpha}, \quad |k_{\xi}(\tau)| + k'_{\xi}(\tau)^2 \leq C_0t^{-\alpha}, \quad \tau \geq 0, \quad (66)$$

for some $\alpha > 2$ and constants c, C, C_0 . Then there is a constant K which depends on k_{ξ} but not on u or T such that, for $T \geq T_0 > 1$,

$$\left| \mathbb{P}\left(\max_{t \in [0, T]} \frac{\xi(t)}{\sqrt{m_{\xi,0}}} \leq u\right) - \exp\left(-\sqrt{\frac{m_{\xi,2}}{m_{\xi,0}}} T \mu(u)\right) \right| \leq K \frac{\log\left(\sqrt{\frac{m_{\xi,2}}{m_{\xi,0}}} T\right)^{1+1/\alpha}}{\left(\sqrt{\frac{m_{\xi,2}}{m_{\xi,0}}} T\right)^{\delta}}, \quad (67)$$

$$\text{with } \mu(u) = \frac{1}{2\pi} e^{-\frac{u^2}{2}}, \quad \delta = \min\{1/2, \inf_{\tau \geq 0} \rho(\tau)\} \quad \text{and} \\ \rho(\tau) = \frac{1}{1 - \frac{1}{m_{\xi,0}^2} k_{\xi}(\tau)^2 + \frac{1}{m_{\xi,0} m_{\xi,2}} k'_{\xi}(\tau) |k'_{\xi}(\tau)|}.$$

When the process ξ is known through its spectral density K_{ξ} , conditions (65) and (66) are met if we have:

$$m_{\xi,4} < \infty, \quad (68)$$

$$K_{\xi} \in C^3, K_{\xi}^{(i)} \text{ and } \omega K_{\xi}^{(j)} \text{ are integrable for } i = 0, 1, 2, 3 \text{ and } j = 0, 1, 2, \quad (69)$$

with $K_{\xi}^{(i)}$ the i -th derivative of K_{ξ} .

Proposition 2 *If a process ξ meets all the conditions of theorem 2, it follows that for all $x_r \in \mathbb{R}$:*

$$\left| \mathbb{P} \left(\max_{t \in [0, T]} \xi(t) \leq x_r \right) - \exp \left(-e^{\frac{a_T^2 - \frac{a_T x_r}{\sqrt{m_{\xi,0}}}}{T}} \right) \right| \leq K \frac{\log \left(2\pi \frac{T}{T_c} \right)^{1+1/\alpha}}{\left(2\pi \frac{T}{T_c} \right)^{\delta}} + \exp \left(-\frac{T}{T_c} \exp \left(-\frac{x_r^2}{2m_{\xi,0}} \right) \right). \quad (70)$$

with $a_T = \sqrt{2 \log \left(\frac{T}{T_c} \right)}$ and $T_c = 2\pi \sqrt{\frac{m_{\xi,0}}{m_{\xi,2}}}$.

Proof (Proof of proposition 2) We have, $\forall x_r \in \mathbb{R}$:

$$a_T^2 - a_T \frac{x_r}{\sqrt{m_{\xi,0}}} + \frac{x_r^2}{2m_{\xi,0}} \geq \min_{x'_r \in \mathbb{R}} a_T^2 - a_T \frac{x'_r}{\sqrt{m_{\xi,0}}} + \frac{x'^2_r}{2m_{\xi,0}} = \frac{a_T^2}{2}. \quad (71)$$

Taking the exponential of right- and left-hand sides gives:

$$\exp \left(-e^{\frac{a_T^2 - \frac{a_T x_r}{\sqrt{m_{\xi,0}}}}{T}} \right) \leq \exp \left(-\frac{T}{T_c} \exp \left(-\frac{x_r^2}{2m_{\xi,0}} \right) \right), \forall x_r \in \mathbb{R}. \quad (72)$$

It follows from this result and theorem 2 with $u = \frac{x_r}{\sqrt{m_{\xi,0}}}$ that:

$$\left| \mathbb{P} \left(\max_{t \in [0, T]} \xi(t) \leq x_r \right) - \exp \left(-e^{\frac{a_T^2 - \frac{a_T x_r}{\sqrt{m_{\xi,0}}}}{T}} \right) \right| \quad (73)$$

$$\leq \left| \mathbb{P} \left(\max_{t \in [0, T]} \xi(t) \leq x_r \right) - \exp \left(-\frac{T}{T_c} \exp \left(-\frac{x_r^2}{2m_{\xi,0}} \right) \right) \right| + \left| \exp \left(-e^{\frac{a_T^2 - \frac{a_T x_r}{\sqrt{m_{\xi,0}}}}{T}} \right) - \exp \left(-\frac{T}{T_c} \exp \left(-\frac{x_r^2}{2m_{\xi,0}} \right) \right) \right| \quad (74)$$

$$\leq K \frac{\log \left(2\pi \frac{T}{T_c} \right)^{1+1/\alpha}}{\left(2\pi \frac{T}{T_c} \right)^{\delta}} + \exp \left(-\frac{T}{T_c} \exp \left(-\frac{x_r^2}{2m_{\xi,0}} \right) \right) \quad (75)$$

□

Application of proposition 2 to extreme-based failure probability approximation

Proposition 3 *We denote by f_{r_E} the probability density function of X_{r_E} and $T_c(x_d, x_p) = 2\pi \sqrt{\frac{m_{y,0}(x_d, x_p)}{m_{y,2}(x_d, x_p)}}$. We assume the following conditions:*

- (1) $\exists K, \alpha, \delta$ such that $\forall x_d, x_p$, the process $\mathcal{Y}(x_d, x_p; \cdot)$ satisfies the conditions of theorem 2,
- (2) $\exists T_1 > 0, T_2 > 0, m_1 > 0$ such that $\forall x_d, x_p, T_1 \leq T_c(x_d, x_p) \leq T_2$ and $m_1 \leq m_{y,0}(x_d, x_p)$,
- (3) $\exists c_1 > 0, c_r > 0$ such that $\forall x, |x| \geq c_1, f_{r_E}(x) \leq c_r \exp \left(-\frac{x^2}{m_1} \right)$.

Then, if $\sqrt{m_1 \log(T)} > c_1$, the error made in the approximation (15) can be bounded as follows:

$$\left| p_E(d) - \mathbb{E}_{X_d, X_p, X_{r_E}} \left[F_{\epsilon} \left(e^{\frac{a_T(X_d, X_p)^2 - \frac{a_T(X_d, X_p)X_{r_E}}{\sqrt{m_{y,0}(X_d, X_p)}}}{T}} \right) \right] \right| \leq K \frac{\log \left(2\pi \frac{T}{T_1} \right)^{1+1/\alpha}}{\left(2\pi \frac{T}{T_2} \right)^{\delta}} + \frac{T_2 + c_r \sqrt{\pi m_1}}{\sqrt{T}}. \quad (76)$$

$$\left| p_E(d) - \mathbb{E}_{X_d, X_p, X_{r_E}} \left[F_{\epsilon} \left(e^{\frac{a_T(X_d, X_p)^2 - \frac{a_T(X_d, X_p)X_{r_E}}{\sqrt{m_{y,0}(X_d, X_p)}}}{T}} \right) \right] \right| \leq \mathbb{E}_{X_d, X_p, X_{r_E}} \left[\left| \mathbb{P}_{\mathcal{Y}} \left(\max_{t \in [0, T]} \mathcal{Y}(X_d, X_p; t) \leq X_{r_E} \right) - \exp \left(-e^{\frac{a_T(X_d, X_p)^2 - \frac{a_T(X_d, X_p)X_{r_E}}{\sqrt{m_{y,0}(X_d, X_p)}}}{T}} \right) \right| \right] \leq \mathbb{E}_{X_d, X_p, X_{r_E}} \left[K \frac{\log \left(2\pi \frac{T}{T_c(X_d, X_p)} \right)^{1+1/\alpha}}{\left(2\pi \frac{T}{T_c(X_d, X_p)} \right)^{\delta}} + \exp \left(-\frac{T}{T_c(X_d, X_p)} \exp \left(-\frac{X_{r_E}^2}{2m_{y,0}(X_d, X_p)} \right) \right) \right] \leq K \frac{\log \left(2\pi \frac{T}{T_1} \right)^{1+1/\alpha}}{\left(2\pi \frac{T}{T_2} \right)^{\delta}} + \mathbb{E}_{X_{r_E}} \left[\exp \left(-\frac{T}{T_2} \exp \left(-\frac{X_{r_E}^2}{2m_1} \right) \right) \right].$$

Proof (Proof of proposition 3)

The two last equations are obtained using successively proposition 2 and assumption (2). Denoting $\alpha_T = \sqrt{m_1 \log(T)}$, it follows from assumption (3):

$$\mathbb{E}_{X_{r_E}} \left[\exp \left(-\frac{T}{T_2} \exp \left(-\frac{X_{r_E}^2}{2m_1} \right) \right) \right] \quad (77)$$

$$= \int_{-\alpha_T}^{\alpha_T} \exp \left(-\frac{T}{T_2} \exp \left(-\frac{x^2}{2m_1} \right) \right) f_{r_E}(x) dx \quad (78)$$

$$+ \int_{\mathbb{R} \setminus [-\alpha_T, \alpha_T]} \exp \left(-\frac{T}{T_2} \exp \left(-\frac{x^2}{2m_1} \right) \right) f_{r_E}(x) dx \quad (79)$$

$$\leq \exp \left(-\frac{T}{T_2} \exp \left(-\frac{\alpha_T^2}{2m_1} \right) \right) + \int_{\mathbb{R} \setminus [-\alpha_T, \alpha_T]} f_{r_E}(x) dx \quad (80)$$

$$\leq \exp \left(-\frac{\sqrt{T}}{T_2} \right) + c_r \int_{\mathbb{R} \setminus [-\alpha_T, \alpha_T]} \exp \left(-\frac{x^2}{m_1} \right) dx \quad (81)$$

$$\leq \frac{T_2}{\sqrt{T}} + c_r \left(\sqrt{\pi m_1} - \sqrt{\pi m_1} \sqrt{1 - \exp \left(-\frac{\alpha_T^2}{m_1} \right)} \right) \quad (82)$$

$$\leq \frac{T_2}{\sqrt{T}} + c_r \sqrt{\pi m_1} \left(1 - \sqrt{1 - \frac{1}{T}} \right) \quad (83)$$

$$\leq \frac{T_2}{\sqrt{T}} + c_r \sqrt{\frac{\pi m_1}{T}}. \quad (84)$$

Equation (82) is obtained considering $I = \int_0^{\alpha_T} \exp \left(-\frac{x^2}{m_1} \right) dx$, then I^2 can be bounded working in polar coordinates. \square

Integral-based failure probability reformulation error

Proposition 4 We denote by f_{r_1} the probability density function of X_{r_1} and for fixed values $x_d, x_p, Z_T(x_d, x_p)$ the random variable $\frac{1}{T} \int_0^T \mathcal{F}(x_d, x_p; t) dt$. We assume the following conditions:

- (1) $\exists c_1 > 0, c_r > 0$ such that $\forall x \geq c_1, f_{r_1}(x) \leq \frac{c_r}{x}$,
- (2) $\exists T_0, c_2 > 0$ such that $\forall x_d, x_p$ and $\forall T > T_0$, $Z_T(x_d, x_p) \geq c_2$ almost surely,

- (3) $\exists c_{\mathcal{F}} > 0$ such that for all x_d, x_p :

$$\int_{\mathbb{R}} |k_{\mathcal{F}}(x_d, x_p; \tau)| d\tau < c_{\mathcal{F}}. \quad (85)$$

Then, if $T > T_0$ and $T > \frac{c_1}{c_2}$, we have:

$$|p_1(d) - \mathbb{E}_{X_d, X_p} [F_{r_1}(T \mathbb{E}_{\mathcal{F}}[\mathcal{F}(X_d, X_p; 0)])]| \leq \frac{c_r}{c_2} \sqrt{\frac{2c_{\mathcal{F}}}{T}}. \quad (86)$$

$$|p_1(d) - \mathbb{E}_{X_d, X_p} [F_{r_1}(T \mathbb{E}_{\mathcal{F}}[\mathcal{F}(X_d, X_p; 0)])]| \quad (87)$$

Proof (Proof of proposition 4)

$$\leq \mathbb{E}_{X_d, X_p, \mathcal{Y}} \left[|F_{r_1}(TZ_T(X_d, X_p)) - F_{r_1}(T \mathbb{E}_{\mathcal{F}}[Z_T(X_d, X_p)])| \right] \quad (88)$$

$$\leq \mathbb{E}_{X_d, X_p, \mathcal{Y}} \left[|TZ_T(X_d, X_p) - T \mathbb{E}_{\mathcal{F}}[Z_T(X_d, X_p)]| \right] \quad (89)$$

$$\max \left(\frac{c_r}{(TZ_T(X_d, X_p))}, \frac{c_r}{(T \mathbb{E}_{\mathcal{F}}[Z_T(X_d, X_p)])} \right) \quad (90)$$

$$\leq \mathbb{E}_{X_d, X_p, \mathcal{Y}} \left[T |Z_T(X_d, X_p) - \mathbb{E}_{\mathcal{F}}[Z_T(X_d, X_p)]| \frac{c_r}{c_2 T} \right] \quad (91)$$

$$\leq \frac{c_r}{c_2} \mathbb{E}_{X_d, X_p} \left[\sqrt{\text{Var}(Z_T(X_d, X_p))} \right]$$

$$\leq \frac{c_r}{c_2} \sqrt{\frac{2c_{\mathcal{F}}}{T}}. \quad (92)$$

Conditions (1), (2) and $T \geq \frac{c_1}{c_2}$ imply equation (89). In (90), we apply the Cauchy-Schwarz inequality and equation (91) follows from:

$$\begin{aligned} \text{Var}(Z_T(x_d, x_p)) &= \frac{1}{T^2} \int_0^T \int_0^T k_{\mathcal{F}}(x_d, x_p; |t - t'|) dt dt' \\ &\leq \frac{2}{T} \int_0^T |k_{\mathcal{F}}(x_d, x_p; \tau)| d\tau. \end{aligned} \quad (92)$$

\square

Proof of the sufficient conditions to reformulate the stationary harmonic oscillator problem

Proof To apply the approximation (15) to the first and second constraints of the oscillator problem we need to show that for all x_d, x_p and for $k = 1, 2$, the following conditions are satisfied:

$$m_{\mathcal{D}^{(k)},0}(x_d, x_p) < \infty, m_{\mathcal{D}^{(k)},2}(x_d, x_p) < \infty \quad (93)$$

$$K_{\mathcal{D}^{(k)}}(x_d, x_p, \cdot) \in C^1, K_{\mathcal{D}^{(k)}}(x_d, x_p, \cdot) \text{ and } K'_{\mathcal{D}^{(k)}}(x_d, x_p, \cdot) \text{ are integrable.} \quad (94)$$

As we have the relation $K_{\mathcal{D}^{(k)}}(x_d, x_p; \omega) = \omega^{2k} K_{\mathcal{D}}(x_d, x_p; \omega) \forall \omega$, to show (93) and (94), it is sufficient to prove that $\omega^i K_{\mathcal{D}}^{(j)}$ is integrable for the appropriate values of i and j where $K_{\mathcal{D}}^{(j)}$ is the j -th derivative of $K_{\mathcal{D}}$. In fact, in our case it is true for all i and j . Indeed, it follows from relation (22) that $K_{\mathcal{D}}(x_d, x_p; \cdot)$ is the product of a rational function (with no real pole) and a Gaussian function. Hence, we can demonstrate that $\forall i \in \mathbb{N}, \forall j \in \mathbb{N}, \omega^i K_{\mathcal{D}}^{(j)}(x_d, x_p; \cdot)$ is integrable. \square

Appendix of section 2

Extreme-based failure probability reformulation

For $j = 1, \dots, n_s$, let us denote $I^j = \bigcup_{i, s_i = s^j} I_i$. Hence, I^j is the union of n^j intervals of length ΔT . For fixed x_d, x_p, x_{r_E} , we have:

$$\mathbb{P}_{\mathcal{Y}} \left(\max_{t \in [0, T]} \mathcal{Y}(x_d, x_p, t) \leq x_{r_E} \right) \quad (95)$$

$$= \mathbb{P}_{\mathcal{Y}} \left(\max_{t \in [0, T]} \sum_{i=1}^{n_T} \mathcal{Y}_i(x_d, x_p, s_i; t) \mathbb{1}_{I_i}(t) \leq x_{r_E} \right) \quad (96)$$

$$= \mathbb{P}_{\mathcal{Y}} \left(\max_{t \in I^1} \sum_{i=1}^{n_T} \mathcal{Y}_i(x_d, x_p, s^1; t) \mathbb{1}_{I_i}(t) \leq x_{r_E}, \dots, \right. \quad (97)$$

$$\left. \max_{t \in I^{n_s}} \sum_{i=1}^{n_T} \mathcal{Y}_i(x_d, x_p, s^{n_s}; t) \mathbb{1}_{I_i}(t) \leq x_{r_E} \right)$$

$$= \prod_{j=1}^{n_s} \mathbb{P}_{\mathcal{Y}_1, \dots, \mathcal{Y}_{n_T}} \left(\max_{t \in I^j} \sum_{i=1}^{n_T} \mathcal{Y}_i(x_d, x_p, s^j; t) \mathbb{1}_{I_i}(t) \leq x_{r_E} \right) \quad (98)$$

$$= \prod_{j=1}^{n_s} \mathbb{P}_{\mathcal{Y}_1, \dots, \mathcal{Y}_{n_T}} \left(\max_{t \in [0, n^j \Delta T]} \sum_{i=1}^{n_T} \mathcal{Y}_i(x_d, x_p, s^j; t) \mathbb{1}_{I_i}(t) \leq x_{r_E} \right). \quad (99)$$

The independence of $\mathcal{Y}_i(x_d, x_p, s_i; \cdot)$ and $\mathcal{Y}_{i'}(x_d, x_p, s_{i'}; \cdot)$ for all $i \neq i'$ is used to obtain equation (98). The last equation results from the fact that $\mathcal{Y}_i(x_d, x_p, s^j; \cdot)$ and $\mathcal{Y}_{i'}(x_d, x_p, s^j; \cdot)$ for $i \neq i'$ are i.i.d processes.

Finally, when ΔT is large, we consider that each term of the product appearing in equation (99) can be approached by

$\mathbb{P}_{\mathcal{Y}_1}(\max_{t \in [0, n^j \Delta T]} \mathcal{Y}_1(x_d, x_p, s^j; t) \leq x_{r_E})$ which leads to approximation (27) since $n^j \Delta T = T p^j$.

Extreme-based failure probability reformulation error

Proposition 5 We denote f_{r_E} the probability density function of X_{r_E} and $T_c(x_d, x_p, s^j) = 2\pi \sqrt{\frac{m_{\mathcal{Y},0}(x_d, x_p, s^j)}{m_{\mathcal{Y},2}(x_d, x_p, s^j)}}$. We assume the following conditions:

- (1) $\exists K, \alpha, \delta$ such that $\forall x_d, x_p, s^j$, the process $\mathcal{Y}_1(x_d, x_p, s^j; \cdot)$ satisfies the conditions of theorem 2,
- (2) $\exists T_1 > 0, T_2 > 0, m_1 > 0$ such that $\forall x_d, x_p, s^j$, $T_1 \leq T_c(x_d, x_p, s^j) \leq T_2$ and $m_1 \leq m_{\mathcal{Y},0}(x_d, x_p, s^j)$,
- (3) $\exists c_1 > 0, c_r > 0$ such that $\forall x, |x| \geq c_1$, $f_{r_E}(x) \leq c_r \exp\left(-\frac{x^2}{m_1}\right)$.

Then, if $\sqrt{m_1 \log(\Delta T)} > c_1$ the error made in equation (28) can be bounded as follows:

$$\begin{aligned} & \left| p_E(d) - \mathbb{E}_{X_d, X_p, X_{r_E}} \left[F_e \left(\sum_{j=1}^{n_s} e^{\frac{a_{T p^j}(x_d, x_p, s^j)^2 - \frac{a_{T p^j}(x_d, x_p, s^j) x_{r_E}}{\sqrt{m_{\mathcal{Y},0}(x_d, x_p, s^j)}}}} \right) \right] \right| \\ & \leq n_s \left(n_T K \frac{\log\left(2\pi \frac{\Delta T}{T_1}\right)^{1+1/\alpha}}{\left(2\pi \frac{\Delta T}{T_2}\right)^\delta} + (n_T + 1) \frac{T_2 + c_r \sqrt{\pi m_1}}{\sqrt{\Delta T}} \right). \end{aligned} \quad (100)$$

Proof (Proof of proposition 5) We introduce the following notations:

$$P_j(T) = \mathbb{P}_{\mathcal{Y}_1} \left(\max_{t \in [0, T]} \mathcal{Y}_1(x_d, x_p, s^j; t) \leq x_{r_E} \right), \quad (101)$$

$$E_j(T) = \exp \left(-e^{\frac{a_T(x_d, x_p, s^j)^2 - \frac{a_T(x_d, x_p, s^j) x_{r_E}}{\sqrt{m_{\mathcal{Y},0}(x_d, x_p, s^j)}}}} \right), \quad (102)$$

$$E_-(T) = \min_{j=1, \dots, n_s} E_j(T), E_+(T) = \max_{j=1, \dots, n_s} E_j(T), \quad (103)$$

$$p^- = \min_{j=1, \dots, n_s} p^j, p^+ = \max_{j=1, \dots, n_s} p^j. \quad (104)$$

For fixed values of x_d, x_p, x_{r_E} , we have $\forall j \in \{1, \dots, n_s\}$:

$$\begin{aligned} & \left| P_j(\Delta T)^{n^j} - E_j(Tp^j) \right| \\ & \leq \left| P_j(\Delta T)^{n^j} - E_j(\Delta T)^{n^j} \right| + \left| E_j(\Delta T)^{n^j} - E_j(Tp^j) \right|. \end{aligned} \quad (105)$$

Besides, using $P_j(\Delta T) \in [0, 1]$, $E_j(\Delta T) \in [0, 1]$, proposition 2 and assumption (2), we obtain:

$$\begin{aligned} & \left| P_j(\Delta T)^{n^j} - E_j(\Delta T)^{n^j} \right| \leq n^j \left| P_j(\Delta T) - E_j(\Delta T) \right| \\ & \leq n_T \left[K \frac{\log \left(2\pi \frac{\Delta T}{T_1} \right)^{1+1/\alpha}}{\left(2\pi \frac{\Delta T}{T_2} \right)^\delta} + \exp \left(-\frac{\Delta T}{T_2} \exp \left(-\frac{x_{r_E}^2}{2m_1} \right) \right) \right]. \end{aligned} \quad (106)$$

Since $E_j(T)$ is a decreasing function with respect to T and that its images are in $[0, 1]$, we have for $n^j > 0$:

$$-E_+(Tp^-) \leq E_j(\Delta T)^{n^j} - E_j(Tp^j) \leq E_+(\Delta T). \quad (107)$$

It follows, with $Tp^- > 1$ (i.e. if $n^j > 0, \forall j$) and applying the preliminary result of proof A.1.1:

$$\begin{aligned} & \left| E_j(\Delta T)^{n^j} - E_j(Tp^j) \right| \leq E_+(\Delta T) \\ & \leq \exp \left(-\frac{\Delta T}{T_2} \exp \left(-\frac{x_{r_E}^2}{2m_1} \right) \right). \end{aligned} \quad (108)$$

We therefore can use equations (106) and (108) to bound the approximation error:

$$\begin{aligned} & \left| p_E(d) - \mathbb{E}_{X_d, X_p, X_{r_E}} \left[F_e \left(\sum_{j=1}^{n_s} e^{a_{Tp^j}(X_d, X_p, s^j)^2 - \frac{a_{Tp^j}(X_d, X_p, s^j) X_{r_E}}{\sqrt{m_{y,0}(X_d, X_p, s^j)}}} \right) \right] \right| \\ & = \left| \mathbb{E}_{X_d, X_p, X_{r_E}} \left[1 - \prod_{j=1}^{n_s} P_j(\Delta T)^{n^j} \right] - \mathbb{E}_{X_d, X_p, X_{r_E}} \left[1 - \prod_{j=1}^{n_s} E_j(Tp^j) \right] \right| \\ & \leq \mathbb{E}_{X_d, X_p, X_{r_E}} \left[\left| \prod_{j=1}^{n_s} P_j(\Delta T)^{n^j} - \prod_{j=1}^{n_s} E_j(Tp^j) \right| \right] \end{aligned} \quad (109)$$

$$\begin{aligned} & \leq n_s \mathbb{E}_{X_d, X_p, X_{r_E}} \left[n_T K \frac{\log \left(2\pi \frac{\Delta T}{T_1} \right)^{1+1/\alpha}}{\left(2\pi \frac{\Delta T}{T_2} \right)^\delta} + (n_T + 1) \exp \left(-\frac{\Delta T}{T_2} \exp \left(-\frac{x_{r_E}^2}{2m_1} \right) \right) \right] \end{aligned} \quad (110)$$

$$\leq n_s \left(n_T K \frac{\log \left(2\pi \frac{\Delta T}{T_1} \right)^{1+1/\alpha}}{\left(2\pi \frac{\Delta T}{T_2} \right)^\delta} + (n_T + 1) \frac{T_2 + c_r \sqrt{\pi m_1}}{\sqrt{\Delta T}} \right) \quad (112)$$

In equation (109), we use the following equalities:

$$\begin{aligned} p_E(d) &= \mathbb{E}_{X_d, X_p, X_{r_E}} \left[1 - \prod_{j=1}^{n_s} \mathbb{P}_{\mathcal{Y}_1, \dots, \mathcal{Y}_{n^j}} \left(\max_{i \in [0, n^j \Delta T]} \sum_{i=1}^{n_T} \mathcal{Y}_i(x_d, x_p, s^j; t) \mathbb{1}_{I_i}(t) \leq x_{r_E} \right) \right] \end{aligned} \quad (113)$$

$$\begin{aligned} &= \mathbb{E}_{X_d, X_p, X_{r_E}} \left[1 - \prod_{j=1}^{n_s} \mathbb{P}_{\mathcal{Y}_1} \left(\max_{i \in [0, \Delta T]} \mathcal{Y}_1(x_d, x_p, s^j; t) \leq x_{r_E} \right)^{n^j} \right]. \end{aligned} \quad (114)$$

Equation (110) holds since, for $a_i, b_i \in [0, 1], n \in \mathbb{N}^*$, if $|a_i - b_i| < c, i = 1, \dots, n$ then $|\prod_{i=1}^n a_i - \prod_{i=1}^n b_i| < nc$. Finally, in equation (112), $\mathbb{E}_{X_{r_E}} \left[\exp \left(-\frac{\Delta T}{T_2} \exp \left(-\frac{x_{r_E}^2}{2m_1} \right) \right) \right]$ is bounded applying the reasoning of proof A.1.2. \square

Proof proposition 1

Proof (Proof of proposition 1) For fixed values x_d, x_p and x , we have:

$$\begin{aligned} & \mathbb{P}_{\mathcal{Y}} \left(\frac{1}{\Delta T} \int_0^T f \left(\sum_{i=1}^{n_T} \mathcal{Y}_i(x_d, x_p, s_i; t) \mathbb{1}_{I_i}(t) \right) dt > x \right) \\ &= \mathbb{P}_{\mathcal{Y}} \left(\frac{1}{\Delta T} \sum_{i=1}^{n_T} \int_{I_i} f(\mathcal{Y}_i(x_d, x_p, s_i; t)) dt > x \right) \end{aligned} \quad (115)$$

$$= \mathbb{P}_{\mathcal{Y}} \left(\sum_{i=1}^{n_T} \frac{1}{\Delta T} \int_0^{\Delta T} f(\mathcal{Y}_i(x_d, x_p, s_i; t)) dt > x \right). \quad (116)$$

The last equality is obtained using the stationarity of the processes $f(\mathcal{Y}_i(x_d, x_p, s_i; \cdot))$ and the independence between $f(\mathcal{Y}_i(x_d, x_p, s_i; \cdot))$ and $f(\mathcal{Y}_{i'}(x_d, x_p, s_{i'}; \cdot))$ for $i \neq i'$. Let $U_{i, \Delta T}$ be the random variable $\frac{1}{\Delta T} \int_0^{\Delta T} f(\mathcal{Y}_i(x_d, x_p, s_i; t)) dt$. It follows from the assumption that $f(\mathcal{Y}_1(x_d, x_p, s^j; \cdot))$ is ergodic for all s^j that:

$$U_{i, \Delta T} \xrightarrow[\Delta \rightarrow +\infty]{\mathbb{P}} u_i, \quad (117)$$

with $u_i = \mathbb{E}_{\mathcal{Y}_i} [f(\mathcal{Y}_i(x_d, x_p, s_i; 0))]$. Using the independence of $U_{i, \Delta T}$ and $U_{i', \Delta T}$ for $i \neq i'$, we deduce that:

$$\sum_{i=1}^{n_T} U_{i,\Delta T} \xrightarrow[\Delta T \rightarrow +\infty]{\mathbb{P}} \sum_{i=1}^{n_T} u_i. \quad (118)$$

Therefore, we have the convergence in distribution:

$$\mathbb{P}_{\mathcal{Y}} \left(\sum_{i=1}^{n_T} \frac{1}{\Delta T} \int_0^{\Delta T} f(\mathcal{Y}_i(x_d, x_p, s_i; t)) dt > x \right) \quad (119)$$

$$\xrightarrow[\Delta \rightarrow +\infty]{\mathbb{P}} \mathbb{1}_{\sum_{i=1}^{n_T} \mathbb{E}_{\mathcal{Y}_i} [f(\mathcal{Y}_i(x_d, x_p, s_i; 0))] > x},$$

for all $x \neq \sum_{i=1}^{n_T} \mathbb{E}_{\mathcal{Y}_i} [f(\mathcal{Y}_i(x_d, x_p, s_i; 0))]$, with

$$\begin{aligned} & \sum_{i=1}^{n_T} \mathbb{E}_{\mathcal{Y}_i} [f(\mathcal{Y}_i(x_d, x_p, s_i; 0))] \\ &= \sum_{j=1}^{n_s} n^j \mathbb{E}_{\mathcal{Y}_1} [f(\mathcal{Y}_1(x_d, x_p, s^j; 0))]. \end{aligned} \quad (120)$$

Integral-based failure probability reformulation error

Proposition 6 We denote f_{r_1} the probability density function of X_{r_1} and for fixed values x_d, x_p :

$$Z_{\Delta T}(x_d, x_p) = \frac{1}{\Delta T} \int_0^T f(\mathcal{Y}(x_d, x_p; t)) dt \quad (121)$$

$$= \frac{1}{\Delta T} \sum_{i=1}^{n_T} \int_{I_i} f(\mathcal{Y}_i(x_d, x_p, s_i; t)) dt, \quad (122)$$

with $k_{\mathcal{F}_1}(x_d, x_p, s_i; \cdot)$ the autocovariance function of the process $\mathcal{F}_1(x_d, x_p, s_i; \cdot)$. We assume that the following assumptions are valid:

- (1) $\exists c_1 > 0, c_r > 0$ such that $\forall x \geq c_1, f_{r_1}(x) \leq \frac{c_r}{x}$,
- (2) $\exists \Delta T_0, \exists c_2 > 0$ such that $\forall x_d, x_p$ and $\Delta T > \Delta T_0$, $Z_{\Delta T}(x_d, x_p) \geq c_2$ almost surely,
- (3) for each state $s^j, \exists c_{\mathcal{F}, s^j} > 0$ such that for all x_d, x_p :

$$\int_{\mathbb{R}} |k_{\mathcal{F}_1}(x_d, x_p, s^j; \tau)| d\tau < c_{\mathcal{F}, s^j}. \quad (123)$$

Then, if $\Delta T > T_0$ and $\Delta T \geq \frac{c_1}{c_2}$, the approximation error made in equation (31) can be bounded as follows:

$$\begin{aligned} & \left| p_1(d) - \mathbb{E}_{X_d, X_p} \left[F_{r_1} \left(T \sum_{j=1}^{n_s} p^j \mathbb{E}_{\mathcal{F}_1} [\mathcal{F}_1(X_d, X_p, s^j; 0)] \right) \right] \right| \\ & \leq \frac{c_r}{c_2} \sqrt{\frac{2n_T}{\Delta T} \sum_{j_1}^{n_s} p^{j_1} c_{\mathcal{F}, s^{j_1}}}. \end{aligned} \quad (124)$$

Proof (Proof of proposition 6) We denote in this proof, for fixed values x_d, x_p :

$$A_i = \int_{I_i} f(\mathcal{Y}_i(x_d, x_p, s_i; t)) dt, \quad (125)$$

$$\mathcal{F}_i(s_i; t) = f(\mathcal{Y}_i(x_d, x_p, s_i; t)), \quad (126)$$

and

$$\begin{aligned} & k_{\mathcal{F}_i, \mathcal{F}_j}(s_i, s_j; t, t') = \mathbb{E}_{\mathcal{F}_i, \mathcal{F}_j} [\mathcal{F}_i(s_i; t) \mathcal{F}_j(s_j; t')] \\ & - \mathbb{E}_{\mathcal{F}_i} [\mathcal{F}_i(s_i; t)] \mathbb{E}_{\mathcal{F}_j} [\mathcal{F}_j(s_j; t')]. \end{aligned} \quad (127)$$

We calculate $\mathbb{E}_{\mathcal{Y}}[A_i]$, $\mathbb{E}_{\mathcal{Y}}[A_i A_j]$, and $\text{Var}_{\mathcal{Y}}(Z_{\Delta T}(x_d, x_p))$ which are used further down in the proof. For the first quantity, we use Fubini's theorem to obtain:

$$\mathbb{E}_{\mathcal{Y}}[A_i] = \Delta T \mathbb{E}_{\mathcal{F}_i} [\mathcal{F}_i(s_i; 0)]. \quad (128)$$

Besides,

$$\begin{aligned} & \mathbb{E}_{\mathcal{Y}}[A_i A_j] \\ &= \mathbb{E}_{\mathcal{Y}} \left[\int_{I_i} \int_{I_j} \mathcal{F}_i(s_i; t) \mathcal{F}_j(s_j; t') dt dt' \right] \end{aligned} \quad (129)$$

$$\begin{aligned} &= \int_{I_i} \int_{I_j} \left(k_{\mathcal{F}_i, \mathcal{F}_j}(s_i, s_j, t, t') \right. \\ & \left. + \mathbb{E}_{\mathcal{F}_i} [\mathcal{F}_i(s_i; t)] \mathbb{E}_{\mathcal{F}_j} [\mathcal{F}_j(s_j; t')] \right) dt dt'. \end{aligned} \quad (130)$$

- if $i \neq j$: by independence of $\mathcal{F}_i(s_i; \cdot)$ and $\mathcal{F}_j(s_j; \cdot)$ we have $k_{\mathcal{F}_i, \mathcal{F}_j}(s_i, s_j; t, t') = 0$ and it follows that $\mathbb{E}_{\mathcal{Y}}[A_i A_j] = \mathbb{E}_{\mathcal{Y}}[A_i] \mathbb{E}_{\mathcal{Y}}[A_j]$,
- if $i = j$: we use the stationarity of $\mathcal{F}_i(s_i, \cdot)$ to obtain the following equalities:

$$\begin{aligned} & \mathbb{E}_{\mathcal{Y}}[A_i^2] \\ &= \int_{I_i} \int_{I_i} \left(k_{\mathcal{F}_i, \mathcal{F}_i}(s_i, s_i, t, t') + \mathbb{E}_{\mathcal{F}_i} [\mathcal{F}_i(s_i; t)]^2 \right) dt dt' \end{aligned} \quad (131)$$

$$= \int_{I_i} \int_{I_i} k_{\mathcal{F}_i}(s_i, |t - t'|) dt dt' + \Delta T^2 \mathbb{E}_{\mathcal{F}_i} [\mathcal{F}_i(s_i; 0)]^2 \quad (132)$$

Let us calculate $\text{Var}_y(Z_{\Delta T}(x_d, x_p))$:

$$\begin{aligned} \text{Var}_y(Z_{\Delta T}(x_d, x_p)) &= \mathbb{E}_y[Z_{\Delta T}(x_d, x_p)^2] - \mathbb{E}_y[Z_{\Delta T}(x_d, x_p)]^2 \end{aligned} \quad (133)$$

$$\begin{aligned} &= \frac{1}{\Delta T^2} \left(\sum_{i=1}^{n_T} \mathbb{E}_y[A_i^2] + 2 \sum_{i < j} \mathbb{E}_y[A_i A_j] \right. \\ &\quad \left. - \sum_{i=1}^{n_T} \mathbb{E}_y[A_i]^2 - 2 \sum_{i < j} \mathbb{E}_y[A_i] \mathbb{E}_y[A_j] \right) \end{aligned} \quad (134)$$

$$= \frac{1}{\Delta T^2} \left(\sum_{i=1}^{n_T} \int_{I_i} \int_{I_i} k_{\mathcal{F}_i}(s_i, |t - t'|) dt dt' \right) \quad (135)$$

$$\leq \frac{2}{\Delta T} \sum_{i=1}^{n_T} \int_0^{\Delta T} |k_{\mathcal{F}_i}(s_i; \tau)| d\tau. \quad (136)$$

To bound the approximation error made in equation (31), the reasoning used in proof A.2 in the stationary case is applied here: assumptions (1), (2) and $\Delta T > \frac{c_1}{c_2}$ imply the second inequality while the Cauchy-Schwarz inequality is used to obtain the third inequality:

$$\left| p_1(d) - \mathbb{E}_{X_d, X_p} \left[F_{r_1} \left(T \sum_{j=1}^{n_s} p^j \mathbb{E}_{\mathcal{F}_1} [\mathcal{F}_1(X_d, X_p, s^j; 0)] \right) \right] \right| \quad (137)$$

$$\begin{aligned} &\leq \mathbb{E}_{X_d, X_p, y} \left[\left| F_{r_1}(\Delta T Z_{\Delta T}(X_d, X_p)) \right. \right. \\ &\quad \left. \left. - F_{r_1}(\Delta T \mathbb{E}_y[Z_{\Delta T}(X_d, X_p)]) \right| \right] \end{aligned} \quad (138)$$

$$\leq \frac{c_r}{c_2} \mathbb{E}_{X_d, X_p, y} \left[|Z_{\Delta T}(X_d, X_p) - \mathbb{E}_y[Z_{\Delta T}(x_d, x_p)]| \right] \quad (139)$$

$$\leq \frac{c_r}{c_2} \mathbb{E}_{X_d, X_p} \left[\sqrt{\text{Var}_y(Z_{\Delta T}(X_d, X_p))} \right] \quad (140)$$

$$\leq \frac{c_r}{c_2} \sqrt{\frac{2n_T}{\Delta T} \sum_{j=1}^{n_s} p^j c_{\mathcal{F}_i, s^j}}. \quad (141)$$

□

Computation of the quantity involved in the integral-based constraint of the oscillator problem

We recall that the random variable $\mathcal{D}_1^{(2)}(x_d, x_p, s^j; 0)$ follows a normal distribution with zero-mean and standard deviation $\sigma_{\mathcal{D}^{(2)}}(x_d, x_p, s^j)$. We denote the latter σ in the following calculations. Thus, we have for the oscillator problem:

$$\begin{aligned} \mathbb{E}_{\mathcal{F}_1} [\mathcal{F}_1(x_d, x_p, s^j; 0)] &= \mathbb{E} \left[\left(|\mathcal{D}_1^{(2)}(x_d, x_p, s^j; 0)| - \rho \right)^+ \right] \\ &= \int_{\mathbb{R}} (|y| - \rho)^+ \frac{1}{\sigma \sqrt{2\pi}} \exp \left(-\frac{y^2}{2\sigma^2} \right) dy. \end{aligned} \quad (142)$$

The integral in the last equation is decomposed into integrals over $(-\infty, -\rho]$ and $[\rho, +\infty)$ and the calculations lead to:

$$\begin{aligned} \mathbb{E}_{\mathcal{F}_1} [\mathcal{F}_1(x_d, x_p, s^j; 0)] &= \sqrt{\frac{2}{\pi}} \sigma \exp \left(-\frac{\rho^2}{2\sigma^2} \right) \\ &\quad + 2\rho \left(\Phi \left(\frac{\rho}{\sigma} \right) - 1 \right), \end{aligned} \quad (143)$$

with Φ the cumulative distribution function of the standard normal distribution.

Declarations

Conflict of interest The authors declare that they have no conflict of interest.

Replication of results The procedure and the flowchart of AK-ECO are provided in Sect. 3 and the implementation is detailed in Sect. 4.

References

- Abdo T, Rackwitz R (1991) A new beta-point algorithm for large time-invariant and time-variant reliability problems. In: Der Kiureghian A, Thoft-Christensen P (eds) Reliability and optimization of structural systems '90. Springer, Berlin, pp 1–12
- Andrieu-Renaud C, Sudret B, Lemaire M (2004) The PHI2 method: a way to compute time-variant reliability. Reliab Eng Syst Saf 84(1):75–86
- Aoues Y, Chateauneuf A (2010) Benchmark study of numerical methods for reliability-based design optimization. Struct Multidiscip Optim 41(2):277–294. <https://doi.org/10.1007/s00158-009-0412-2>
- Baudin M, Dutfoy A, Iooss B, Popelin A (2016) OpenTURNS: an industrial software for uncertainty quantification in simulation. Springer, Cham, pp 1–38. https://doi.org/10.1007/978-3-319-11259-6_64-1
- Berman S (1991) Spectral conditions for sojourn and extreme value limit theorems for Gaussian processes. Stoch Process Appl 39(2):201–220
- Bourinet J (2018) Reliability analysis and optimal design under uncertainty—focus on adaptive surrogate-based approaches.

- Habilitation à diriger des recherches, Université Clermont Auvergne, <https://tel.archives-ouvertes.fr/tel-01737299>
- Buhmann MD (2003) Radial basis functions: theory and implementations. Cambridge Monographs on Applied and Computational Mathematics, Cambridge University Press. <https://doi.org/10.1017/CBO9780511543241>
- Burmester S, Vaz G, Gueydon S, el Moutar O (2020) Investigation of a semi-submersible floating wind turbine in surge decay using CFD. *Ship Technol Res* 67(1):2–14
- Cousin A, Garnier J, Guiton M, Munoz Zuniga M (2021) Chance constraint optimization of a complex system: application to the fatigue design of a floating offshore wind turbine mooring system. WCCM-ECCOMAS2020 https://www.scipedia.com/public/Cousin_et_al_2021a
- Du X, Chen W (2004) Sequential optimization and reliability assessment method for efficient probabilistic design. *J Mech Des* 10(1115/1):1649968
- Dubourg V (2011) Adaptive surrogate models for reliability analysis and reliability-based design optimization. Theses, Université Blaise Pascal - Clermont-Ferrand II. <https://tel.archives-ouvertes.fr/tel-00697026>
- El Hami A, Radi B, Huang C (2017) Overview of structural reliability analysis methods—Part II: sampling methods. Uncertainties and reliability of multiphysical systems I (Optimization and Reliability). 10.21494/ISTE.OP.2017.0116
- Hasselmann DE, Duncel M, Ewing JA (1980) Directional wave spectra observed during JONSWAP 1973. *J Phys Oceanogr* 10(8):1264–1280
- Hawchar L (2017) Développement de méthodes fiabilistes dépendant du temps pour l'analyse de durabilité des structures: application au problème de conception fiabiliste dépendant du temps. PhD thesis, Nantes
- Hawchar L, El Soueidy C, Schoefs F (2018) Global kriging surrogate modeling for general time-variant reliability-based design optimization problems. *Struct Multidiscip Optim* 58(3):955–968
- Cand Helbert D, Dupuy Carraro L (2009) Assessment of uncertainty in computer experiments from universal to Bayesian Kriging. *Appl Stoch Model Bus Ind* 25:99–113. <https://doi.org/10.1002/asmb.743>
- Hu Y, Lu Z, Wei N, Zhou C (2020) A single-loop kriging surrogate model method by considering the first failure instant for time-dependent reliability analysis and safety lifetime analysis. *Mech Syst Signal Process* 145:106963
- Hu Z, Du X (2015) Mixed efficient global optimization for time-dependent reliability analysis. *J Mech Des* 137(5):0151401. <https://doi.org/10.1115/1.4029520>
- Huchet Q, Matrand C, Beaurepaire P, Relun N, Gayton N (2019) AK-DA: an efficient method for the fatigue assessment of wind turbine structures. *Wind Energy* 22(5):638–652. <https://doi.org/10.1002/we.2312>
- Jensen H, Valdebenito M, Schüller G (2008) An efficient reliability-based optimization scheme for uncertain linear systems subject to general gaussian excitation. *Comput Methods Appl Mech Eng* 198(1):72–87
- Jerez D, Jensen H, Beer M (2022) Reliability-based design optimization of structural systems under stochastic excitation: an overview. *Mech Syst Signal Process* 166:108397
- Jiang C, Wang D, Qiu H, Gao L, Chen L, Yang Z (2019) An active failure-pursuing kriging modeling method for time-dependent reliability analysis. *Mech Syst Signal Process* 129:112–129
- Jiang C, Qiu H, Li X, Chen Z, Gao L, Li P (2020) Iterative reliable design space approach for efficient reliability-based design optimization. *Eng Comput* 36(1):151–169
- Kanda J (2021) Applications of total expected cost concept to various decision making situations. *Struct Saf* 88:102038
- Kratz MF, Rootzén H (1997) On the rate of convergence for extremes of mean square differentiable stationary normal processes. *J Appl Probab* 34(4):908–923. <https://doi.org/10.2307/3215006>
- Krige D (1951) A statistical approach to some basic mine valuation problems on the witwatersrand. *J S Afr Inst Min Metall* 52(6):119–139
- Kroetz H, Moustapha M, Beck A, Sudret B (2020) A two-level kriging-based approach with active learning for solving time-variant risk optimization problems. *Reliab Eng Syst Saf* 203:107033
- Labeyrie J (1990) Stationary and transient states of random seas. *Mar Struct* 3(1):43–58. [https://doi.org/10.1016/0951-8339\(90\)90020-R](https://doi.org/10.1016/0951-8339(90)90020-R)
- Le Cunff C, Ryu S, Heurtier JM, Duggal AS (2008) Frequency-domain calculations of moored vessel motion including low frequency effect. In: International Conference on Offshore Mechanics and Arctic Engineering, vol Volume 1: Offshore Technology, pp 689–696, 10.1115/OMAE2008-57632, https://asmedigitalcollection.asme.org/OMAE/proceedings-pdf/OMAE2008/48180/689/4570979/689_1.pdf
- Leadbetter M, Lindgren G, Rootzén H (1983) Extremes and related properties of random sequences and processes. Springer series in statistics. Springer, Berlin
- Leira BJ, Igland RT, Baarholm GS, Farnes KA, Percy D (2005) Fatigue safety factors for flexible risers based on case specific reliability analysis. In: International Conference on Offshore Mechanics and Arctic Engineering, vol 24th International Conference on Offshore Mechanics and Arctic Engineering, vol 2, pp 211–217. <https://doi.org/10.1115/OMAE2005-67432>, https://asmedigitalcollection.asme.org/OMAE/proceedings-pdf/OMAE2005/41960/211/4560688/211_1.pdf
- Lemaire M, Chateaneuf A, Mitteau J (2009) Structural reliability. Wiley Online Library, New York
- Li J, Chen J (2019) Solving time-variant reliability-based design optimization by PSO-t-IRS: a methodology incorporating a particle swarm optimization algorithm and an enhanced instantaneous response surface. *Reliab Eng Syst Saf* 191:106580
- Li X, Han X, Chen Z, Ming W, Cao Y, Ma J (2020) A multi-constraint failure-pursuing sampling method for reliability-based design optimization using adaptive Kriging. *Eng Comput*. <https://doi.org/10.1007/s00366-020-01135-3>
- Liang J, Mourelatos Z, Tu J (2008) A single-loop method for reliability-based design optimization. *Int J Prod Dev*. <https://doi.org/10.1504/IJPD.2008.016371>
- Lindgren G (2012) Stationary stochastic processes: theory and applications. Chapman and Hall/CRC. <https://doi.org/10.1201/b12171>
- Ling C, Lu Z, Zhu X (2019) Efficient methods by active learning Kriging coupled with variance reduction based sampling methods for time-dependent failure probability. *Reliab Eng Syst Saf* 188:23–35
- Lopez R, Beck A (2012) Reliability-based design optimization strategies based on FORM: a review. *J Braz Soc Mech Sci Eng* 34(4):506–514
- Madsen H, Krenk S, Lind N (2006) Methods of structural safety. Courier Corporation, Chelmsford
- McKay M, Beckman R, Conover W (2000) A comparison of three methods for selecting values of input variables in the analysis of output from a computer code. *Technometrics* 42(1):55–61
- Moan T, Gao Z, Ayala-Uraga E (2005) Uncertainty of wave-induced response of marine structures due to long-term variation of extratropical wave conditions. *Mar Struct* 18(4):359–382
- Moustapha M, Sudret B (2019) Surrogate-assisted reliability-based design optimization: a survey and a unified modular framework. *Struct Multidiscip Optim* 60(5):2157–2176. <https://doi.org/10.1007/s00158-019-02290-y>
- Moustapha M, Marelli S, Sudret B (2022) Active learning for structural reliability: survey, general framework and benchmark. *Struct Saf*. <https://doi.org/10.1016/j.strusafe.2021.102174>

- Nocedal J, Wright SJ (2006) Numerical optimization, 2nd edn. Springer, New York
- Papoulis A (1991) Probability, random variables, and stochastic processes. Communications and signal processing. McGraw-Hill, New York
- Powell MJD (1994) A direct search optimization method that models the objective and constraint functions by linear interpolation. Springer, Dordrecht, pp 51–67. https://doi.org/10.1007/978-94-015-8330-5_4
- Rasmussen CE (2004) Gaussian processes in machine learning. Springer, Berlin, pp 63–71. https://doi.org/10.1007/978-3-540-28650-9_4
- Robertson A, Jonkman J, Masciola M, Song H, Goupee A, Coulling A, Luan C (2014) Definition of the Semisubmersible Floating System for Phase II of OC4. 10.2172/1155123. Technical Report NREL/TP-5000-60601
- Rossi RR (2005) A review of fatigue curves for mooring lines. In: International Conference on Offshore Mechanics and Arctic Engineering, vol 24th International Conference on Offshore Mechanics and Arctic Engineering: Volume 1, Parts A and B, pp 1097–1104. 10.1115/OMAE2005-67583. https://asmedigitalcollection.asme.org/OMAE/proceedings-pdf/OMAE2005/41952/1097/4560624/1097_1.pdf
- Santner TJ, Williams BJ, Notz WI, Williams BJ (2018) The design and analysis of computer experiments. Springer, New York
- Shang X, Ma P, Yang M, Chao T (2021) An efficient polynomial chaos-enhanced radial basis function approach for reliability-based design optimization. Struct Multidiscip Optim 63(2):789–805. <https://doi.org/10.1007/s00158-020-02730-0>
- Shi Y, Lu Z, Huang Z, Xu L, He R (2020) Advanced solution strategies for time-dependent reliability based design optimization. Comput Methods Appl Mech Eng 364:112916
- Sobol' IM (1967) On the distribution of points in a cube and the approximate evaluation of integrals. USSR Comput Math Math Phys 7(4):86–112. [https://doi.org/10.1016/0041-5553\(67\)90144-9](https://doi.org/10.1016/0041-5553(67)90144-9)
- Stieng L, Muskulus M (2020) Reliability-based design optimization of offshore wind turbine support structures using analytical sensitivities and factorized uncertainty modeling. Wind Energy Sci 5(1):171–198
- Teixeira R, Nogal M, O'Connor A (2021) Adaptive approaches in metamodel-based reliability analysis: a review. Struct Saf 89:102019
- Torii A, Lopez R, Miguel L (2016) A general RBDO decoupling approach for different reliability analysis methods. Struct Multidiscip Optim 54(2):317–332
- Tu J, Choi K, Park Y (1999) A new study on reliability-based design optimization. J Mech Des 121(4):557–564
- Valdebenito M, Jensen H, Schuëller G, Caro F (2012) Reliability sensitivity estimation of linear systems under stochastic excitation. Comput Struct 92–93:257–268
- Valdebenito M, Jensen H, Labarca A (2014) Estimation of first excursion probabilities for uncertain stochastic linear systems subject to gaussian load. Comput Struct 138:36–48
- Det Norske Veritas (2013) Design of floating wind turbine structures. Offshore Standard DNV-OS-J103
- Vorpahl F, Schwarze H, Fischer T, Seidel M, Jonkman J (2013) Offshore wind turbine environment, loads, simulation, and design. Wiley Interdisc Rev Energy Environ 2(5):548–570
- Wang Z, Chen W (2016) Time-variant reliability assessment through equivalent stochastic process transformation. Reliab Eng Syst Saf 152:166–175
- Wang Z, Li H, Chen Z, Li L, Hong H (2020) Sequential optimization and moment-based method for efficient probabilistic design. Struct Multidiscip Optim 62(1):387–404. <https://doi.org/10.1007/s00158-020-02494-7>
- Wiener N (1938) The homogeneous chaos. Am J Math 60(4):897–936
- Wu Z, Chen Z, Chen G, Li X, Jiang C, Gan X, Gao L, Wang S (2021) A probability feasible region enhanced important boundary sampling method for reliability-based design optimization. Struct Multidiscip Optim 63(1):341–355
- Yang M, Zhang D, Han X (2020) Enriched single-loop approach for reliability-based design optimization of complex nonlinear problems. Eng Comput. <https://doi.org/10.1007/s00366-020-01198-2>
- Youn BD, Choi KK, Park YH (2003) Hybrid analysis method for reliability-based design optimization. J Mech Des 125(2):221–232. <https://doi.org/10.1115/1.1561042>
- Zhang H, Aoues Y, Lemosse D, de Cursi E (2020) A single-loop approach with adaptive sampling and surrogate Kriging for reliability-based design optimization. Eng Optim. <https://doi.org/10.1080/0305215X.2020.1800664>
- Zhang J, Xiao M, Gao L (2020) A new local update-based method for reliability-based design optimization. Eng Comput. <https://doi.org/10.1007/s00366-020-01019-6>
- Zhang Z, Deng W, Jiang C (2021) A PDF-based performance shift approach for reliability-based design optimization. Comput Methods Appl Mech Eng 374:113610

Publisher's Note Springer Nature remains neutral with regard to jurisdictional claims in published maps and institutional affiliations.